THESIS FOR THE DEGREE OF LICENTIATE OF ENGINEERING

Modeling and Simulation of a Multi Phase Semi-batch Reactor

Anna Nyström

CHALMERS | GÖTEBORG UNIVERSITY

Department of Mathematical Sciences
Chalmers University of Technology and Göteborg University
Göteborg, Sweden 2007

This work was partly supported by:
Akzo Nobel Functional Chemicals

Modeling and Simulation of a Multi Phase Semi-batch Reactor
Anna Nyström

NO 2007:17
ISSN 1652-9715
Department of Mathematical Sciences
Chalmers University of Technology and Göteborg University
SE-412 96 Göteborg
Sweden
Telephone +46 (0)31 772 1000

Printed in Göteborg, Sweden 2007

Modeling and Simulation of a Multi Phase Semi-batch Reactor

Anna Nyström

Department of Mathematical Sciences
Chalmers University of Technology
Göteborg University

Abstract

The operation of an industrial semi-batch reactor is modeled and the flow of one reactant is investigated. In the reactor a strongly exothermic polymerization reaction takes place followed by a slightly exothermic reaction, and the objective is to minimize the duration of the operation of the process. Various operational as well as quality and safety related constraints have to be met during the batch. The complete process model is derived from measurements, first principles, and reasoning about effects on molecular level.

This work has been performed in cooperation between Akzo Nobel Functional Chemicals and Chalmers. We have increased the knowledge of one semi batch process and tried to improve the production of thickeners by modeling the production process with the aid of mathematics. A better understanding of the underlying principles including the chemical reaction heat, energy transfer and the control system has been gained.

The process model is simulated using MATLAB and SIMULINK. The optimization is made through investigations of manually chosen EO profiles and simulations.

Piecewise constant EO profiles with up to three constant plateaus and varying levels have been used. Simulations show that a 5 % increase in total batch time is possible, using a profile with two plateaus as in the original, but with 20 % higher levels and no delay.

A 10 % shorter batch time than today is possible using a profile with three different plateau levels. However, in this a profile, a large portion of the EO is added prior to the wanted reaction temperature is reached, which may result in a worsened end product quality. In order to decide which profiles are acceptable, more research about the effect of the reaction temperature used on the end product quality is needed.

Keywords: semi-batch reactor, modeling, simulation, optimization

Till farmor

Preface

This thesis is the final result of the post-graduate program in industrial mathematics organized by ECMI, the European Consortium for Mathematics in Industry. The ECMI post-graduate program is designed to improve the participants' interdisciplinary skills and to promote and nourish the use of mathematical methods in industry.

The work has been performed in close collaboration with the industrial partner Akzo Nobel Functional Chemicals, Stenungsund, Sweden. The financial support from Akzo Nobel is greatly acknowledged.

I am grateful to my supervisor Professor Michael Patriksson for all discussions and for the guidance through the art of writing mathematics.

I would like to thank my assistant supervisors Dr. Åsa Lindgren at Akzo Nobel and Professor Urban Grén, for your interest in the subject, support and encouragement.

I also want to thank Professor Bengt Andersson at Chemical Reaction Engineering for all discussions which have been very useful for the progress of the work.

I thank all my colleges at the department, and especially Karin Kraft and Christoffer Cromvik for all support and enjoyable coffee breaks.

Finally I am very thankful for all support and love from my husband Jonas, and my children Erika, Gustav and Viktor, and to my sister Maria for her never ending encouragement.

Contents

1 Introduction

In this work, the operation of an industrial semi-batch reactor is studied and optimized. In the reactor a strongly exothermic polymerization reaction takes place followed by a slightly exothermic reaction, and the objective is to minimize the duration of the batch time. Various operational as well as quality and safety related constraints have to be met during the batch. The work has been performed in cooperation between Akzo Nobel Functional Chemicals and Chalmers.

What in chemical engineering is called optimization of batch reactors, fall under the mathematical branch of optimization of dynamical systems. Another common name is optimal control. In the first section we try to unite the chemical and mathematical terminology, by first giving an overview of the chemical engineering area and then describing the mathematics, and dynamic optimization in particular.

Knowledge about cellulose ethers and their chemistry is valuable for understanding for the process model, and we begin with a discussion about this in Section 1.1. Thereafter follows a short description of batch processes, their use and properties. The objectives of the thesis conclude the first section. Optimization of batch processes is reviewed in Section 2, as well as dynamic optimization in general and typical dynamic optimization methods.

In Section 3 we describe the process, and the modeling steps towards a final mathematical model, using first principles and empirical equations. We argue why some physical aspects are considered and some are discarded at this stage. We also point out where further investigations can be done in order to increase the accuracy of the model.

In Section 4, the optimization problem is formulated and the control vector is parameterized. A manual optimization is performed, by choosing EO profiles and running simulations, and the results are discussed.

We conclude the work and point out interesting future work in Section 5.

1.1 Cellulose ethers

Cellulose ethers are named after, and based on, cellulose — a natural and renewable polymer. Cellulose is the most common chemical compound in organic nature and the chief component of wood and plant fibres.

Cellulose ethers are used as additives in such diverse industries as food, paint, oil recovery, paper, cosmetics, pharmaceuticals, adhesives, printing, agriculture, ceramics, textiles, detergents and building materials. Cellulose ethers improve the product quality in these industries and act as thickeners, water retention agents, suspending aids, protecting colloids, film formers or thermoplastics in such different products as dispersion paints, drilling muds, ice cream, tablet coatings, wallpaper paste and tile adhesive.

Cellulose ethers are obtained by reacting cellulose with different substituents such as for instance methyl, ethyl, and hydroxyethyl. This etherification process makes the product water soluble.

Cellulose is a polysaccharide composed of individual anhydroglucose units (AHG) which are held together by β-1,4 glycoside linkages which make cellulose a long rigid molecule. The hydrogen bonds within the cellulose molecule give a stiffness to the single molecule, while the hydrogen bonds between molecules are responsible for the formation of crystalline areas, which make cellulose non-water soluble despite its hydrophilic character. These bonds are broken by treatment with sodium hydroxide. This causes the cellulose fibers to swell through electrostatic repulsion between the ionized hydroxyl groups, as well as through hydration of these groups. The structure of the crystalline areas are expanded allowing the hydroxyl groups to be transformed into alcoholate. This cellulose alcoholate is termed alkali cellulose.

The strong attractive forces between cellulose chains due to interchain hydrogen bonds will be greatly reduced by alkylating a portion of the -OH groups, thereby preventing hydrogen bonds. Such chemical modification results in significantly changed characteristics with regard to solubility, surface activity, chemical resistance and enzyme resistance. The properties of the end product depend on the length of the cellulose chain, on the type and amount of substituents as well as the distribution of substituents along the chain.

By combining these substituents in different ways it is possible to customize the properties for different applications. For example, the substitution with both ethyl and hydroxyethyl, resulting in the cellulose ether EHEC (Ethyl HydroxyEthyl Cellulose), gives the product a surface-active character, which stabilizes small air bubbles when added to cement and gypsum-based systems. EHEC also improves water retention, suitable consistency and improved adhesion in these systems. The simplified chemical structure of EHEC is displayed in Figure 1.

When producing EHEC in a batch reactor, alkali cellulose is reacted first with ethylene oxide and then with ethyl chloride under pressure and increased temperature, Figure (2).

1.2 Batch and semi-batch processes

In order to understand the properties of a batch and semi-batch system, we discuss the differences between continuous and batch processes.

In continuous processes, raw materials are fed and products removed on a continuous basis. Hence, the conditions within the process are mainly the same over time. Variations in feed composition, plant utilities, catalyst activities and other variables occur, but normally these changes are either about an average or exhibit a gradual change over an extended period of time.

In a batch process, the materials are loaded, the process is initiated, and as the reactions are completed, the products are removed. Hence, the conditions within the process are changing. The technology for making a given product is contained in the product recipe that is specific to that product [37]. The recipes are typically based on heuristics and experience. By the term semi-batch we means processes in which some parts are continuous but others are of batch type. For instance, in semi-batch operation a gas of limited solubility may be fed in gradually as it is used up.

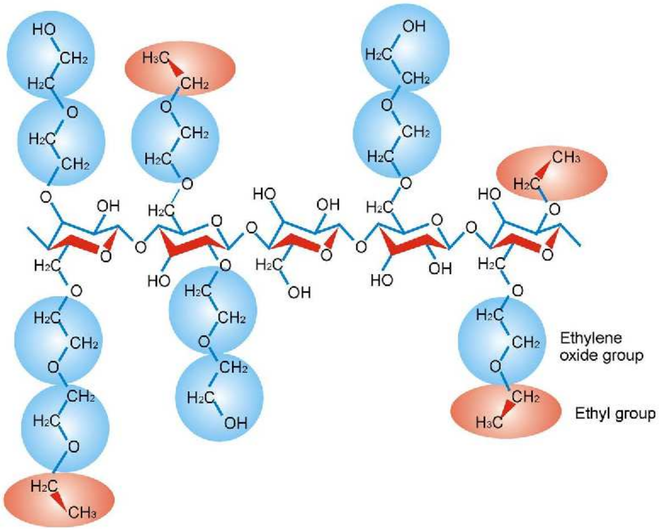

Figure 1: Possible structural elements of EHEC.

Batch reactors are popular in practice because of their flexibility with respect to the duration of the chemical reaction and to the kinds and amounts of reactions that they can process. Generally batch processes are less safe, both for people and the environment, and the variations are larger than in continuous processes [27]. In industry, batch and semi-batch reactors are often used in the production of fine chemicals, specialties, polymers and other high value products. Batch reactors are typically used when production volumes are low, when there are many processing steps, when isolation is required for reasons of sterility or safety, and when the materials involved are difficult to handle. The plants are often small and flexible, and the raw material and the products are expensive, but they can also be used in large volumes. They are primarily employed for relatively slow reactions of several hours duration, since the down time for filling, emptying and cleaning the equipment may be about one hour.

Chemical processes are modeled dynamically using differential algebraic equations (DAEs), consisting of differential equations that describe the dynamic behavior of the system, such as mass and energy balances, and algebraic equations that describe physical and thermodynamic relations. Batch systems are difficult to study numerically due to the fact that steady state is never reached. In addition, chemical processes are typically nonlinear. In order to improve their performance and safety conditions, batch reactors generally require knowledge about the dynamic behavior, for instance through a mathematical description of the kinetics. The development and validation of detailed dynamic models are often quite expensive, and there is,

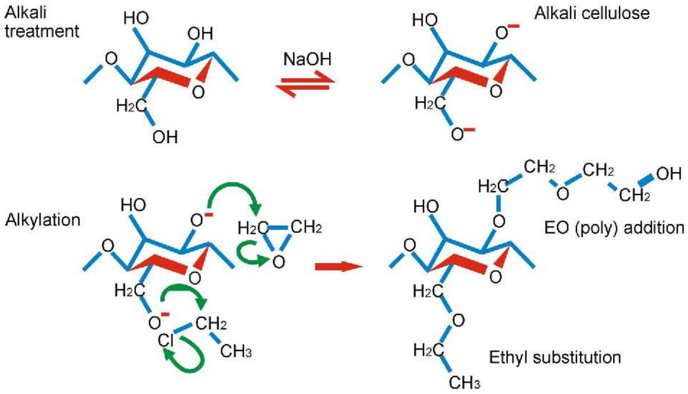

Figure 2: Chemical reactions when producing ethyl hydroxy ethylcellulose, EHEC

in contrast to continuous processes which have been rigorously studied, a limited availability of detailed dynamic models. For bulk chemicals, the cost of developing models is rarely taken. Instead, the operators use experience to adjust the process periodically. Verwater-Lukszo [37] addresses this issue.

Make it work and don't worry about why is a common way of thinking in industry. Another philosophy is *Don't change anything that is functioning, otherwise you will end up with problems*. The background to these attitudes is that process engineers normally assume that nothing changes in the process. But in real life this is not the case. Contaminants and impurities resulting from chemical side reactions, unreacted starting materials, and so on, are difficult to avoid, and may dramatically change the properties of the product. These contaminants vary from batch to batch. On top of this, equipment gets old. Stops and disturbances in production cost tremendously and compared to new investments, process optimization is a more cost effective way to enhance production.

1.3 Objectives

The objectives in this thesis are two-fold: first, to increase the knowledge and acceptance in chemical industry for using mathematics in the daily work. We try to do this by showing that also small models can be used to gain knowledge about a semibatch process. The semibatch process considered works reasonably well today, and the temperature and pressure profiles are more or less based on experience. Measurements during batches show that the existing equipment has some difficulties to follow the current set point profiles, especially during the second temperature rise. Also, measurements on the resulting product have shown that the prevailing settings gives a product with larger variations of the properties between batches than wanted. If the temperature can be better controlled the variation between batches can be decreased, with a more homogeneous product as a result. In this work, we investigate how different flow profiles affect the total batch time, without changing the slopes in the set temperature profile and keeping the existing equipment. To do this we formulate a mathematical model of the process.

The second objective with this work is of an academic nature, namely to provide an overview of the methods that can be used for applying dynamic optimization to an industrial example in the chemical batch industry. We focus on model based process optimization, in which the optimization is performed using a mathematical model of the process, and neither process optimization by control optimization (which is when the control system is optimized around a stable working point) nor process optimization performed through multivariate analysis and design of experiments, are discussed.

2 Process optimization

2.1 Optimization of batch reactors in the process industry

Starting as a technology in applications, mainly through operations research in the sense of optimizing complex systems and phenomena, optimization gradually became an area of academic interest in the time period after World War 2. Especially mathematicians, physicians and economists contributed to the foundations. In the process systems engineering, on the contrary, it has evolved from an academic interest into a technology that has and continues to make a significant impact in industry. The increased competition in industry makes process optimization a natural choice for reducing production costs, improving product quality and reducing product variability. Often the objective in optimization of batch and semi-batch reactors is economic in nature, for instance reducing operational costs. Typically, operational decisions such as temperature and feed flow rates are determined from the optimization problem, and various operational constraints are considered. Often when polymerization is done in semi-batch reactors this results in the consideration of multiple objective functions that are conflicting and non-commensurate in nature [11, 14, 24, 26, 39]. The practice of, and optimization challenges in, batch chemical industry is addressed by Bonvin et al. [6]. Overviews of the research on optimization of batch reactors until 1998 can be found in Rippin [30] and Bonvin [5]. Generally, the industry has a limited acceptance for optimization based techniques for the determination of operational profiles: to develop and validate detailed dynamic models is often considered too expensive to be motivated.

Optimization of a batch reactor can be performed in different stages. When designing an industrial process, it is important to compute the optimal operating conditions (typically in laboratory in advance [26]) required to produce products with specific properties: a recipe. The next step is to implement these conditions in an optimal way in the industrial unit for a safe, stable and efficient production, making sure that the effect of disturbances is repressed.

If information about the product and process is given during the production, this data can be used to perform an on-line optimization. There may be problems, partly because of the lack of accurate online sensors for the measurements of the properties [26, 32]. If uncertainties are present these have to be taken care of [13, 25, 31, 33, 34]. When models are available, for instance MPC or NMPC (Model Predictive Control/nonlinear MPC) can be used to improve the production.

In other processes, the verification of the quality of the end product is possible only after the entire batch has been processed; for instance, this is the case when the reaction occurs under high pressure, fast reactions or other extreme conditions. Then online optimization is impossible, and off-line optimization is the choice. A model or a simulator, maybe made beforehand for other purposes, can be used to optimize the process off-line, with the advantage that the process never need to be stopped or the ordinary scheme interrupted.

Two different types of models are used in the literature: shortcut models, used for determining the reactor temperature profile, and detailed models, used for optimizing the operating conditions for an already designed batch reactor. Typically systems with one phase present are studied, mostly liquid [2, 12], or systems in which only one reactant is present in the gas phase [17, 18]. In our case, three phases are present, which makes the problem much more complicated.

Batch reactors are used on laboratory, pilot and production scale. Many results about the optimization of batch reactors can be found in the open literature on laboratory scale, in different areas: distillation [7, 22], crystallization [10, 9], free-radical polymerization [39], polymerization [11], etoxylation, and in food industry [15]; fed-batch fermentation and thermal sterilization. Some work concerns isothermal reactions [36]. A typical problem is that to find an optimal temperature profile that minimizes the time, which also is the problem in this work, under the constraints of known reaction rates and mass balance. Another common optimization problem is the maximal yield problem. Some applications of optimization of batch reactors to pilot or production scale are found in [1] and [35]. In the latter reference, experimental results are given for a small pilot plant with focus on an improved temperature control. Others report applications to production scale reactors, but do not present results for the operation of the reactor [16, 20]. For production scale reactors, simplified models of the kinetics are typically used, possibly in combination with mass balances [1, 20].

In Abel et al. [1] the conventional reactor temperature T_0 is constant and it is assumed that the reactor content has already been heated to the temperature T_0 prior to the feeding phase, in contrast to our study, where also heating the reactor content is taken into account in the mathematical model. Moreover, they study a non-equilibrium two-phase system with all reactions taking place in liquid phase. Here we deal with *three* phases, and it is not known where the reactions take place. As in our work, the dynamics of the cooling system is neglected, meaning that we assume that the control system is fast enough in order to implement the new trajectories. Of course, this has to be checked. In Abel et al. sensitivity information for the objective function and the constrained states with respect to the free optimization variables is given simultaneously in each iteration from the integration program used. In this study, we do not have access to this information.

Other articles more similar to our study are Khuu et al. [18] and [17], where the EO reaction with nonylphenol is studied. The reaction takes place in liquid phase with nitrogen and EO in gas phase. Also here, the reactor content is preheated to the reaction temperature before EO is added. The kinetics are well known from the literature, and the reactor pressure is directly affected by the EO concentration, which makes the pressure modeling simpler than in our case. Compared to our work, differences are that the heat loss to the surroundings is taken into account in their model by a linear term, and that they use a simultaneous method for solving the optimization problem; see Section 2.3 for a description of this methodology.

In contrast to optimization of continuous processes, where one single set of optimal operating conditions is determined, optimization of batch and semi-batch systems requires the calculation of time dependent trajectories, due to the dynamic behavior. Hence, optimization of these reactors requires the use of dynamic optimization techniques.

2.2 Dynamic optimization

Before we discuss solution methods of dynamic optimization, it is useful to present a classification of problem types. This classification of optimization problems is independent of the solution methods, which are discussed in the next section.

Optimization problems can first be classified in terms of continuous or discrete variables. For continuous problems an important distinction is whether the problem is differentiable or not. Another important distinction, for both types of problems, is whether the problem is convex or nonconvex, since the latter may give rise to local minima different from the global optima. Discrete/continuous optimization problems can be represented in the following general algebraic form:

$$\begin{aligned}
&\text{minimize} \quad f(x,y), && \text{(1a)}\\
&\text{s.t.} \quad h(x,y) = 0, && \text{(1b)}\\
&\qquad g(x,y) \leq 0, && \text{(1c)}\\
&\qquad x \in X, y \in \{0,1\}^m, && \text{(1d)}
\end{aligned}$$

where f is the objective function, $h(x,y) = 0$ are the equations that describe the performance of the system (material balances, production rates, etc.), and $g(x,y) \leq 0$ are the inequalities that define the specifications or constraints for feasible plans and schedules. The variables $x \in \mathbb{R}^n$ are continuous and generally correspond to state variables with some limitations described by X, while $y \in \mathbb{R}^m$ are the discrete variables, which generally are restricted to take on 0-1 values to define for instance the assignments of equipment and sequencing of tasks. When the problem includes uncertainty, this gives rise to stochastic optimization problems. If the system (1b) describes a dynamic model, in discrete problems this gives rise to multi period optimization problems, while for the case of continuous problems this gives rise to optimal control problems that generally involve DAE systems. In Biegler and Grossman [4] a general review on optimization in process systems engineering is provided, emphasizing nonlinear programming (NLP), mixed-integer nonlinear programming (MINLP), dynamic optimization, and optimization under uncertainty.

A general continuous optimal control problem, with the control variable u, and state variable x, is written as follows:

$$\begin{aligned}
&\text{minimize} \quad f = \int_0^{t_f} L(x(t),u(t),t)dt + \phi(x(t_f)), && \text{(2a)}\\
&\text{s.t.} \quad h\left(\frac{dx}{dt}(t), x(t), u(t), t\right) = 0, && \text{(2b)}\\
&\qquad g(x(t),u(t),t) \leq 0, && \text{(2c)}\\
&\qquad x(t) \in X, u(t) \in U, && \text{(2d)}\\
&\qquad x(0) \in X_0, x(t_f) \in X_f, && \text{(2e)}\\
&\qquad t \in [0,t_f]. && \text{(2f)}
\end{aligned}$$

For optimal control problems, a distinction is whether the final time t_f is free or fixed (known beforehand). Assuming the duration of the process to be finite (otherwise the optimization is carried out in an infinite-dimensional space), the free end time problem can be transformed into a sequence of fixed end time problems by, instead of having one objective function f and one constraint function h, having a sequence of cost functions f_k and constraint functions h_k, parameterized by the duration k. Similarly, we have to assume that we have a sequence of subsets U_k, and so on.

Minimum-time problems are optimal control problems in which it is required to go from some initial state to some terminal state in a minimum amount of time:

$$\text{minimize} \quad t_f, \tag{3a}$$

$$\begin{aligned} \text{s.t.} \qquad h(\dot{x}(t), x(t), u(t), t) &= 0, && (3b)\\ g(x(t), u(t), t) &\leq 0, && (3c)\\ x \in X, u(t) &\in U, && (3d)\\ x(0) \in X_0, x(t_f) &\in X_f, && (3e)\\ t &\in [0, t_f]. && (3f) \end{aligned}$$

This is the type of optimization problem we have in this work.

2.3 Dynamic optimization methods

A continuous optimal control problem such as (2) can be solved either by Calculus of variations (indirect methods) or by applying some level of discretization that converts the problem into a discretized problem (direct methods) [3]. If the optimization will be performed in combination with an existing simulator, a direct sequential method is the first choice.

2.3.1 Indirect methods

The variational approach, resulting in indirect methods, is based on the solution of the first order necessary conditions for optimality, that are obtained from Pontryagin's Maximum Principle [29]. For problems without the inequality constraints, (2c), the optimality conditions can be formulated as a set of differential-algebraic equations, and solving these equations require the attention to the boundary conditions. Normally, the state variables are given as initial conditions and the adjoint variables as final conditions, whence the result is a Two Point Boundary Value Problem (TPBVP). For problems with bounds like (2c), the additional multipliers and complementary conditions result in a combinatorial problem which is difficult to solve even for small problems. This TPBVP can be solved with different approaches, including single shooting, invariant embedding, multiple shooting, or some discretization method such as collocation on finite elements or finite differences; see the survey [8] for more information.

2.3.2 Direct methods

In direct methods, the problem is parameterized by a finite number of parameters, transforming the continuous optimization problem to a discretized optimization problem. These methods use NLP solvers, and can be divided into two groups; sequential and simultaneous strategies. A general drawback of both is that the quality of the solution depends on the discretization.

Sequential methods are also called Control Vector Parametrization (CVP) [1]. The control vector u is discretized (into piecewise constant, piecewise linear or piecewise polynomial), and the dynamic equation $\dot{x} = f(x, u)$ is solved explicitly in each optimization step, with well-known integration, which means that also a non-optimal solution is feasible. Figure 3 illustrates the iterations between the NLP solver and the DAE solver.

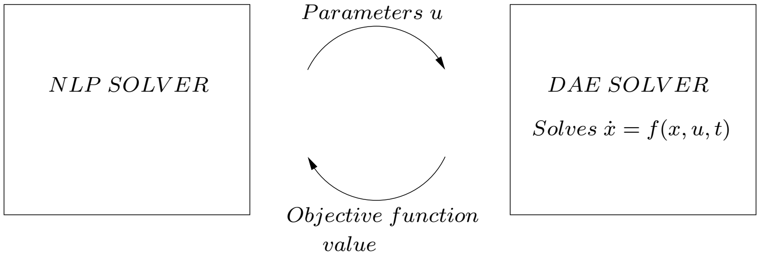

Figure 3: In sequential methods, each iteration the NLP solver sends values of the control parametrization to the DAE solver, which solves the equation $\dot{x} = f(x, u)$. This produces a value of the objective function which is used by the NLP solver to find the optimal parameters in the control parametrization.

The accuracy of the numerical interpolation used in solving the problem is directly related to the accuracy of the optimization problem [28]. Advantages of these methods are that they can handle rather large problems without large scale optimization techniques, and that a non-optimal solution is feasible. These methods run into problems, if the optimization algorithm requires gradient information, because standard DAE solvers are not usually written to provide parametric sensitivities of the solution, or, if provided, they might not be accurate enough for highly nonlinear models. An existing simulator may well be used to solve the DAE [2].

In simultaneous methods all variables are discretized, and the dynamic equation is solved implicitly, simultaneously with the optimization problem. This results in large nonlinear optimization problems that require specialized methods. The simultaneous methods couple the DAE to the optimization problem, and the DAE is solved only once at the optimal point. An advantage of these methods is that they are applicable to general problems. The methods are advantageous for problems with path constraints and also for problems where instabilities occur for a range of inputs, since they are able to suppress unstable nodes by enforcing the appropriate boundary conditions. A disadvantage is the need to solve large nonlinear problems. The fact that the control variables are discretized at the same level as the state variables rises questions about the convergence to the solution of the original continuous optimization problem. In Biegler et al. [3] references to a number of studies, where this is discussed, can be found and also references where it is shown that the Karush-Kuhn-Tucker (KKT) conditions of the simultaneous NLP can be made consistent with the optimality conditions of the variational problem. Nevertheless, these consistency properties do not guarantee convergence to the solution to the infinite dimensional optimal control problem. A review of simultaneous methods can be found in [8]. Examples of methods that can be used to solve the NLP are Sequential Quadratic Programming (SQP) [12], single shooting, multiple shooting [21] and direct shooting method (which is a bridge between direct and indirect methods), invariant embedding, global orthogonal collocation, orthogonal collocation on finite elements [7, 39], and moving finite elements [3].

2.3.3 Other methods

Simulated annealing [10, 22], which is a form of stochastic optimization proposed by Kirpatrick et al. [19], is an attractive global optimization method due to its simplicity. It can surmount the problems of being trapped into local minima since the search in the solution space for global optimum is random. The random nature of the optimization means that some ′uphill′ moves are allowed in the course of minimization of an objective function. In addition, no derivatives are needed for the optimization and this reduces or even eliminates the problem of non-convergence. However, the use of simulated annealing can in continuous optimization be very time consuming.

Work has also been done in which Artificial Neural Network (ANN) models are combined with prior qualitative knowledge [23]. A disadvantage with ANN is that the network can only be used for one product. Also training of the network demands a large amount of input and output data with variations. In reality, these variations are avoided, which means that old process data does not contain enough outliers.

3 Modeling and simulation

In order to optimize the batch time, we need a mathematical description of the process. The plant managers want the model to be simple and at the same time to capture the most important physical aspects of the process; it should also be easy to include more advanced physical properties if needed. In this work, the model is used to study different strategies for the process, in the meaning of shortest possible time, keeping safety and other conditions within certain limits.

A chemical process can mathematically be described by heat and mass balances, resulting in a differential-algebraic equation (DAE) system. For this we need a description of the process, which follows in Section 3.1. In Section 3.2 we set up the DAE system, consisting of mass and heat balances and equations that describe the control system, including constraints. In the text, we motivate why some aspects are regarded while some are not. The main approximation is the averaging of the reactor content, whose effect is discussed below and in Section 3.6.

3.1 Process description

Akzo Nobel uses a semi batch reactor when producing EHEC, which is used as thickener in water based systems. The production occurs under high pressure in a stirred reactor, with exothermal reactions. First, ground cellulose and aqueous NaOH are loaded into the empty reactor and stirred. The NaOH reacts with hydroxyl groups of the cellulose molecule, forming alkali cellulose. Ethyl chloride (EC) is then loaded until a sufficiently high pressure is reached.

The first reaction step starts when liquid EO is added by spraying, according to the schematic in Figure 4, in which the scaled mass flow of EO added to the reactor is plotted over time. An initial addition of EO, at constant high level for a short period

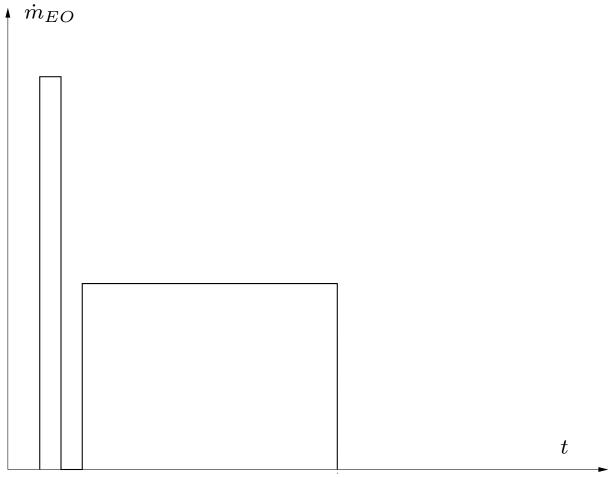

Figure 4: The EO addition profile according to which the process is run today at Akzo Nobel.

of time (the first plateau), starts the batch. This is followed by a second plateau at a lower level but for a longer time period. The resulting reaction, mainly between alkali cellulose and EO, is strongly exothermal, which means that heat is produced. Efficient stirring is essential for a satisfactory product distribution, as well as heat transfer from the reactor.

Simultaneously as the first EO plateau starts, the temperature is raised from the starting temperature T_0 to the first reaction temperature T_1, see Figure 5. Just before this temperature is raised, the second EO plateau starts. The temperature is held constant at temperature T_1 for a certain time, by cooling the reactor. Then the temperature is raised again and when temperature T_2 is reached, the EC-reaction dominates, also producing heat. After some time the temperature is lowered, by cooling through the jacket and the condenser, and the reactor is unloaded and cleaned. The product is then cleaned and further processed.

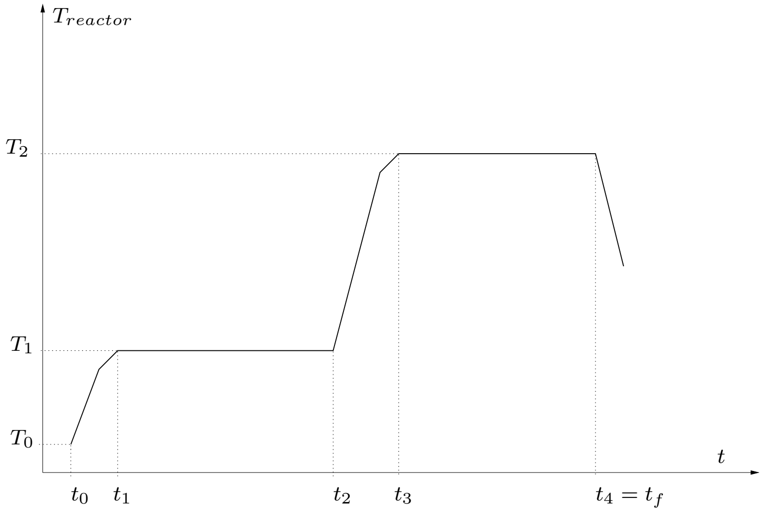

Figure 5: The temperature profile according to which the process is run today at Akzo Nobel.

The participating reactions are exothermal, thereby causing the need for cooling during the reaction steps, but also heating is necessary during temperature rises: from T_0 to T_1 and from T_1 to T_2 of the batch cycle. Today one batch takes a couple of hours to run, including loading and unloading.

Today the system is run according to old 'hands-on' experience and it works reasonably well. Comparisons between batches are regularly made with the aid of multivariate analysis, considering temperatures, pressure, product quality etc. The deviations are larger than wanted.

Investigations regarding chemical reactions and reaction rates have been made, but no detailed investigation regarding reaction heat. Data is available in the form of snapshots for every 15 seconds. Batch data is available for several years back, including measurements on reactor temperatures (measured at three locations; the average is used), reactor pressure, temperatures (in and out of) and flow through the jacket and the condenser, the mass of added materials, values of controllers, etc.

Below the system controlling the reactor temperature is described, followed by a discussion about the phases inside the reactor and the reactions occurring in the reactor.

3.1.1 The temperature control system

The temperature in the reactor is controlled by two separate systems: the condenser and the jacket. The water in the jacket is circulated through a cold water inlet, through a heat exchanger to the reactor jacket, passing by an outlet where surplus water can be removed to keep pressure constant on the way back to the cold water inlet, cf. Figure 6. The flow through the jacket system, F_{jacket}, is kept constant at a high level with a pump. In the heat exchanger steam is used as heating agent and the temperature of the cold, so called raw, water varies slightly during the year. The flow in the jacket is much higher than in the condenser. PID-regulators control the temperature of the jacket flow and the flow through the condenser, and the temperature and the pressure in the reactor is measured.

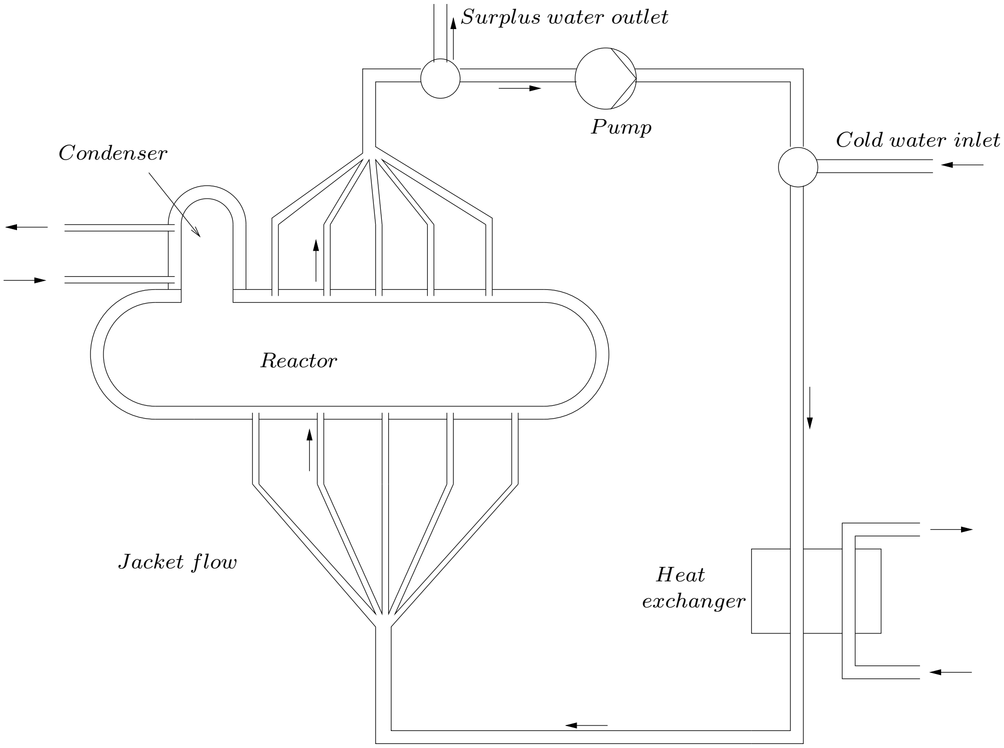

Figure 6: A process schematic, showing the jacketed reactor with the condenser to the left. The jacket system consists of the reactor jacket, outlet, pump, inlet and heat exchanger.

Typical profiles of set temperature, measured reactor and jacket temperatures, as well as measured reactor pressure, and calculated concentrations of EO and EC are shown in Figure 7.

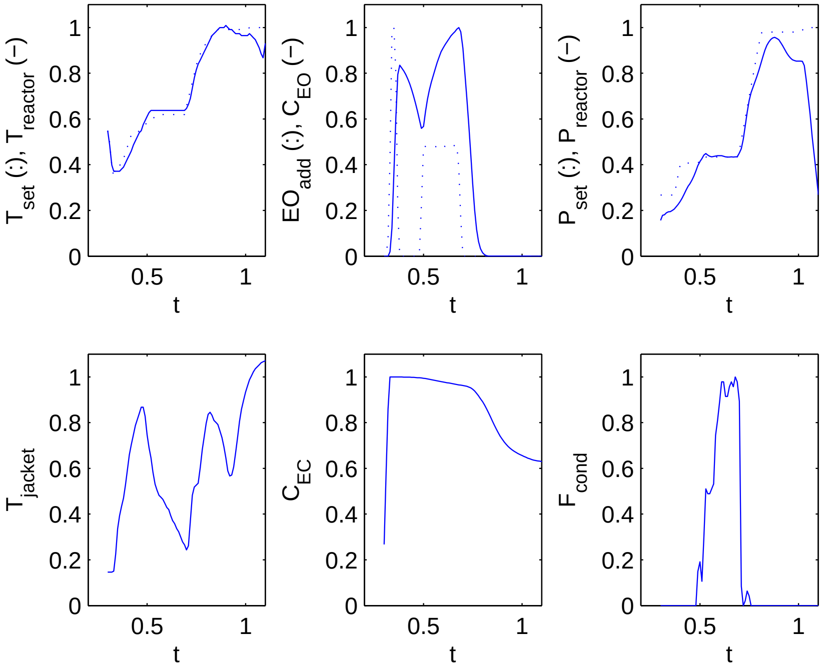

Figure 7: An example of profiles from a typical real batch, with scaled axes. The concentrations of c_{EO} and c_{EC} is calculated and the other variables are measured.

3.1.2 Phases in the reactor

The reactor is constructed such that when the pressure is raised (mainly by adding EC), only temperature and pressure is measurable and the phases in the reactor can only be estimated theoretically.

As mentioned above, the reactor temperature is measured at three different places, and the temperatures differ somewhat. Below the condenser the temperature is a few degrees lower than at the other two places. This temperature decrease can be described by the following. The state of the system is chosen such that the condensation of gases in the condenser is effective. Assuming that no solid material is transported into the condenser, this means that in the condenser, both liquid and gas are present. Part of the gas condenses, causing a pressure drop, thereby leaving energy (heat of condensation) to the condenser wall, and the condensate pours down toward the stirred reactor. As the drops enter the stirred reactor material, it (possibly first absorbs into the cellulose particles, after which it) vaporizes again, which requires energy from the surroundings, causing a temperature decrease. By stirring the reactor, this temperature decrease slowly evens out through the material.

Hence, at least close to the condenser, all three phases (gas, liquid and solid) are present. This affects two things: where the reactions take place, and the time scale of heat transfer from the reaction to the surroundings. These, in turn, affect the local reaction rate and concentrations, as well as the local temperature.

3.1.3 Chemical reactions

In this process, alkali cellulose [the result of Reaction (4), shown below], is reacted with EO, resulting in a chain of ethylene oxide (EO) molecules with an alcoxylate ion at the end, represented in Reaction (5). Ethyl chloride (EC) then reacts either with this alcoxylate ion or directly with alkali cellulose, according to Reactions (6) and (7). Different lengths of the EO-chain give different properties of the end product; the temperature in the reactor, in turn, determines the length of the chain. The reactions are described by:

$$\begin{aligned} \mathrm{Cellulose-OH+OH^-} &\longrightarrow \mathrm{Cellulose-O^-+H_2O} && (4)\\ \mathrm{Cellulose-O^-+nEO} &\longrightarrow \mathrm{Cellulose-O-(EO)_n^-} && (5)\\ \mathrm{Cellulose-O-(EO)_n^-+EC} &\longrightarrow \mathrm{Cellulose-O(EO)_n-Et+Cl^-} && (6)\\ \mathrm{Cellulose-O^-+EC} &\longrightarrow \mathrm{Cellulose-O-Et+Cl^-} && (7) \end{aligned}$$

Reaction (4) initializes the reaction, Reaction (5) is a propagation reaction, and Reactions (6) and (7) terminate the reaction chain.

We assume Reactions (4)–(7) to be the dominating reactions. Other bi-reactions, like EO reacting with other EO-molecules or with water molecules, are neglected.

Reaction (4) is very fast and occurs before EC is completely added to the reactor. In addition, the reaction between alkali cellulose and EC is very slow at low temperatures in the beginning of the process. Thus, the following reactions are not affected by the rate of this reaction and we consider the addition of EO as the starting time for the model.

3.2 Mass and heat balances

In this section we state the differential algebraic equations needed to describe the system, by formulating heat and mass balances. The equations are valid for all $t \in [0, \infty)$.

We start with an overall mass balance over the reactor, with units kg:

$$m_{tot}(t) = \sum_{\substack{All \\ Substances\, i}} m_i(0) + \int_0^t \dot{m}_{EO,add}(\tau)\, d\tau. \qquad (8)$$

In this equation, the first term in the right-hand side represents the initial mass, and the second term describes the (mass) addition to the reactor. As mentioned above, only ethylene oxide (EO) is added to the reactor and nothing is removed from the reactor during a batch.

3.2.1 Overall heat balance

We also need an overall heat balance, with units kJ/s, over the reactor:

$$\frac{1}{V}\frac{\partial}{\partial t}\sum_{\substack{All\\ Substances\ i}} m_i(t)C_{V,i}(T_r(t))T_r(t) = Q_{in}(t) - Q_{out}(t) + Q_{react}(t). \tag{9}$$

The left-hand side describes the accumulation term which is the sum of accumulated heat in each substance in the reactor. The reactor volume V is constant over the batch time and the pressure P is changing over time, which is why we use the heat capacity $C_V(T)$ instead of $C_P(T)$ (which is used when the pressure is constant). Values of C_V [kJ/mol, K] are not available for most species, whereas values of C_P are. For ideal gases, the heat capacity C_V depends only on the temperature, and $C_V(T) = C_P(T) - R$, where R is the ideal gas constant. For solids, $C_V(T) = C_P(T)$ holds. Empirical equations, giving the temperature dependence of $C_P(T)$, are available for many pure species in Perry's Chemical Engineers' Handbook, [27]; they often take the form

$$C_{P,i}(T) = A_i + B_iT + C_iT^2 + D_iT^{-2}.$$

We do not know exactly which substances are present in the reactor because of the bi-reactions occurring, cf. Section 3.1.3. We also do not know much about the phases in the reactor, and even less about the properties of these substances. Values of the heat capacity are known for many pure substances, such as EO and EC and NaOH(aq), but as soon as mixing is regarded, these values change somewhat. The heat capacity for pure cellulose depend, among other things, on the density (for instance fibres or ground powder of different sizes) and the moisture content. Hence, using temperature dependent heat capacities for each present substance is a rather complicated way to express the system.

To make a simple model of the system, we treat the system globally, hence regarding the material inside the reactor as one homogeneous (mass) average compound, with material properties being the average of the compounds'. The average is taken over the whole reactor including the condenser. In order to make a simple model, we need to find approximate, steady state, values for the properties of this average compound, such as heat capacity C_P, heat transfer coefficients k_{cond} and k_{jacket}, through trials and parameter estimation; see Section 3.5. For a more thorough discussion about the effects of the averaging, see Section 5.

As temperature and pressure of this average compound, we use the (time variable) average reactor temperature and reactor pressure, which can be approximated by the measured values in the real reactor. This averaging gives a simpler accumulation term:

$$\frac{\partial}{\partial t}(m_{tot}(t)C_{P,tot}T_r(t)) = Q_{in}(t) - Q_{out}(t) + Q_{react}(t)$$
$$= Q_{EO,add}(t) - Q_{jacket}(t) - Q_{cond}(t) + Q_{react}(t). \tag{10}$$

Developing the left-hand side, assuming $C_{P,tot}$ is constant, gives

$$\frac{\partial}{\partial t}(m_{tot}(t)C_{P,tot}T_r(t)) = C_{P,tot}T_r(t)\frac{\partial}{\partial t}m_{tot}(t) + C_{P,tot}m_{tot}(t)\frac{\partial}{\partial t}T_r(t). \tag{11}$$

Inserting this into Equation (9) gives

$$\frac{\partial}{\partial t}T_r(t) = \frac{1}{C_{P,tot}m_{tot}(t)}[-\dot{m}_{tot}(t)C_{P,tot}T_r(t)+$$
$$Q_{EO,add}(t) - Q_{jacket}(t) - Q_{cond}(t) + Q_{react}(t)]. \tag{12}$$

3.2.2 Heat transfer through addition of EO

EO is added to the reactor by spraying at temperature T_{add}. We assume that EO vaporizes immediately as it enters the reactor, which can be described by two effects: vaporization, followed by a temperature rise of the gas from the addition temperature T_{add} to the reactor temperature T_r. We discard the pressure change due to vaporization; this is acceptable since the pressure changes are very fast (more or less instant) and in this first model we only consider phenomena in time scales larger than about 1 minute. The heat content in the EO-addition is given by Equation (13) below, where $\dot{n}_{add}$ is the molar flow of EO to the reactor, in $mole/min$:

$$Q_{EO,add}(t) = \dot{n}_{add}(t)[\Delta H_{vap}^{EO}(T_{add}) + C_{P,EO}^{gas}(T_r)T_r(t) - C_{P,EO}^{gas}(T_{add})T_{add}]. \tag{13}$$

The heat of vaporization, ΔH_{vap}^{EO}, is given by Equation (14) below, in units $kJ/mole$, with constants in Table 1, and the specific heat for EO, $C_{P,EO}^{gas}$, in units $kJ/mole, K$, is given in Reaction (15), where the constants are given in Table 2, from [38]:

$$\Delta H_{vap}^{EO}(T) = A(1 - \frac{T}{B})^C, \tag{14}$$
$$C_{P,EO}^{gas}(T) = a_0 + a_1T + a_2T^2 + a_3T^3 + a_4T^4. \tag{15}$$

Table 1: Constants used in Equation (14) for vaporization of EO, where T is given in Kelvin.

A	36.474
B	469.15
C	0.3770

Table 2: Constants used in Equation (15) to calculate the specific heat for gaseous ethylene oxide. T is given in Kelvin.

a_0	$30.8271\,10^{-3}$
a_1	$-7.6041\,10^{-6}$
a_2	$3.2347\,10^{-7}$
a_3	$-3.275\,10^{-10}$
a_4	$9.7271\,10^{-14}$

3.2.3 Jacket heat transfer

Heat is transported from and to the reactor through the jacket and from the reactor through the condenser. The heat transfer from gas phase to a wall differs a lot from the transfer from a liquid phase to a wall, as well as from the transfer from a solid phase to a wall. Since we do not know the relations between the different phases in the reactor, or even which phases are present, as above we treat the content as one average compound. Trials at the laboratory, made by Akzo Nobel prior to this study, have shown that an about three times larger amount of EC added to the cellulose, compared to what is used in the process today, is needed to visually observe any liquid phase. Consequently, we assume that all EC and EO is either absorbed by the cellulose or in the gas phase in the reactor.

We estimate the overall heat transfer coefficient k from real batches in a pilot reactor, for the jacket transfer and for the condenser transfer; see Section 3.5 for a further description of the parameter estimation. The jacket is regarded as an ideal tube reactor. Since the flow through the jacket is very high, and the temperature difference between inflow temperature and outflow temperature is less than $5K$ (compared to $50K$ over one batch), this means that the average temperature $\overline{T}_{jacket} = (T_{in} + T_{out})/2$ can be used as an approximation.

The heat transfer Q_{jacket} from the homogeneous average compound material to the jacket water can be described through a heat balance over the jacket, treating the jacket as a point sink in the reactor. The water flow through the jacket is constant: $F_{jacket} = 100\ m^3/h$. Compared to the chosen accuracy in time, the heat transfer through the wall is fast enough to be neglected. By the same reason, we also assume that no heat is accumulated in the reactor wall. Hence, the temperature of the water flowing in the jacket is $\overline{T}_{water,bulk} = \overline{T}_{jacket}$, which can be measured and controlled within certain limits. Using an overall heat transfer coefficient, k_{jacket}, and letting A_{jacket} be the heat transfer area (the reactor surface area excluding the condenser), we get Equation (16) below (the units are kJ/s):

$$\begin{aligned} Q_{jacket} &= k_{jacket} A_{jacket} (T_{reactor}(t) - \overline{T}_{water,bulk}(t)) \\ &= k_{jacket} A_{jacket} (T_{reactor}(t) - \overline{T}_{jacket}(t)). \end{aligned} \tag{16}$$

3.2.4 Condenser heat transfer

The corresponding situation for heat transfer through the condenser wall is slightly more complex. From the reactor point of view, we treat the condenser as a point sink in the reactor, in the same manner as treating the reactor content as one homogeneous compound. But from the condenser point of view, we need to regard the large temperature difference, up to $90K$, between in- and outflow temperatures of the condenser, as follows.

The flow of water through the condenser, F_{cond}, varies over time (we assume incompressible liquid), while the temperature of the water coming in to the system, $T_{cond,in}$ is constant and known. As above, we assume that no heat is accumulated in the condenser wall, thus getting

$$\begin{aligned} Q_{cond} &= k_{cond}A_{cond}(T_{gas,bulk} - T_{water,bulk}) \\ &= k_{cond}A_{cond}(T_{reactor}(t) - \overline{T}_{cond}(t)), \end{aligned} \tag{17}$$

where k_{cond} is the estimated overall heat transfer coefficient, and A_{cond} is the heat transfer area, (that is, the effective condenser area. To deal with the fact that both k_{cond} and $\overline{T}_{cond}$ are unknown, we treat the water side of the heat exchanger as a tube of flowing water, see Figure 8, and use the average temperature as the condenser temperature. In future work, we recommend that other averages, such as logarithmic, are studied also. It therefore follows that

$$\overline{T}_{cond} = \frac{T_{cond,in} + T_{cond,out}}{2}. \tag{18}$$

A heat balance over the condenser, using Equations (17) and (18), gives a new expression for the temperature out of the condenser:

$$0 = F_{cond}C_P(T_{cond,in} - T_{cond,out}) + Q_{cond}$$

$$\Longrightarrow$$

$$T_{out} = \frac{(2F_{cond}C_P - k_{cond}A_{cond})T_{cond,in} + 2k_{cond}A_{cond}T_{reactor}}{2F_{cond}C_P + k_{cond}A_{cond}}. \tag{19}$$

This expression is then used in Equation (17), together with Equation (18).

3.2.5 Reaction heat

Since the reactions involved are exothermal, heat is produced. The amount of this heat is given by:

$$Q_{reaction}(t) = \Delta H_{EO}r_{EO}(t) + \Delta H_{EC}r_{EC}(t). \tag{20}$$

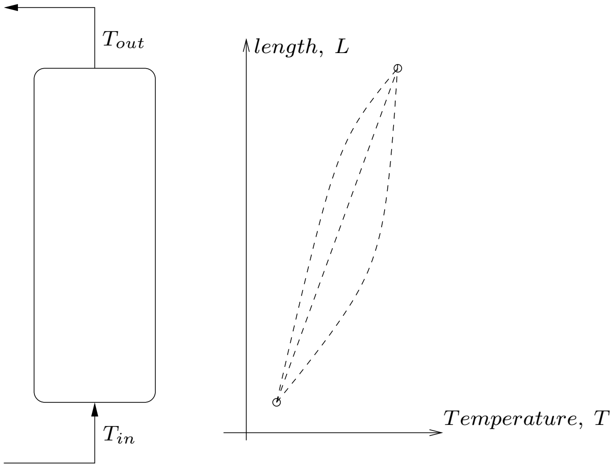

Figure 8: The temperature of incoming water to the condenser may differ a lot from the outgoing water temperature. Without a thorough investigation of the condenser, we do not know the temperature profiles along the length of the condenser, at any of the sides. This uncertainty is handled by using the average temperature.

In this equation, ΔH_i is the heat of reaction for reaction i in $[kJ/mol\ min]$. Trials have been done in a pilot reactor, to establish the reaction heat ΔH_i for the two reactions and the overall specific heat $C_{P,tot}$ of the reactor content. The temperature independent values are estimated while regarding the reactor content as one homogenous average compound. It should be pointed out that the pilot reactor differs from the industrial reactor in the temperature control system: there is no condenser present in the former.

In order to describe the reaction heat in Equation (20), we also need expressions for the reaction rates. Reaction rates are available from test trials in laboratory scale and pilot scale, with concentrations in $[mol/mol\ AGU]$, where AGU is a short-hand for anhydroglucose unit:

$$\frac{\partial c_{\mathrm{EO}}}{\partial t} =- r_{EO'} = -k_{EO}(T)c_{\mathrm{EO}}, \tag{21a}$$

$$\frac{\partial c_{\mathrm{EC}}}{\partial t} =- r_{EC'} = -k_{EC}(T)c_{\mathrm{EC}}c_{\mathrm{RO}^-}. \tag{21b}$$

We use the subscript EO for Reaction (5), and subscript EC for Reaction (6). The c_j:s are total concentrations in the reactor, which means that the formulas do not reveal or consider where reactions take place, or if the molecules have to be transported in liquid or inside a porous particle. By RO^- we mean an activated cellulose ion, see Reaction (4). The reaction constants $k_{EO}(T)$ and $k_{EC}(T)$ are derived from the

Arrhenius equation, where T is the reaction temperature:

$$k_{EO}(T(t)) = A_1 e^{-\frac{E_1}{T(t)}}, \tag{22a}$$

$$k_{EC}(T(t)) = A_2 e^{-\frac{E_2}{T(t)}}. \tag{22b}$$

The entities A_i and E_i, $i = 1, 2$, are constants and the activation energies for the reactions, respectively.

3.3 Control system

The control system of the reactor consists of a jacket, in which the temperature is controlled against the reactor temperature, and a condenser. The cooling effect of the condenser is controlled by varying the flow through the condenser while the temperature of the inflowing water is constant, and this flow is controlled against the reactor pressure. See Figure 9.

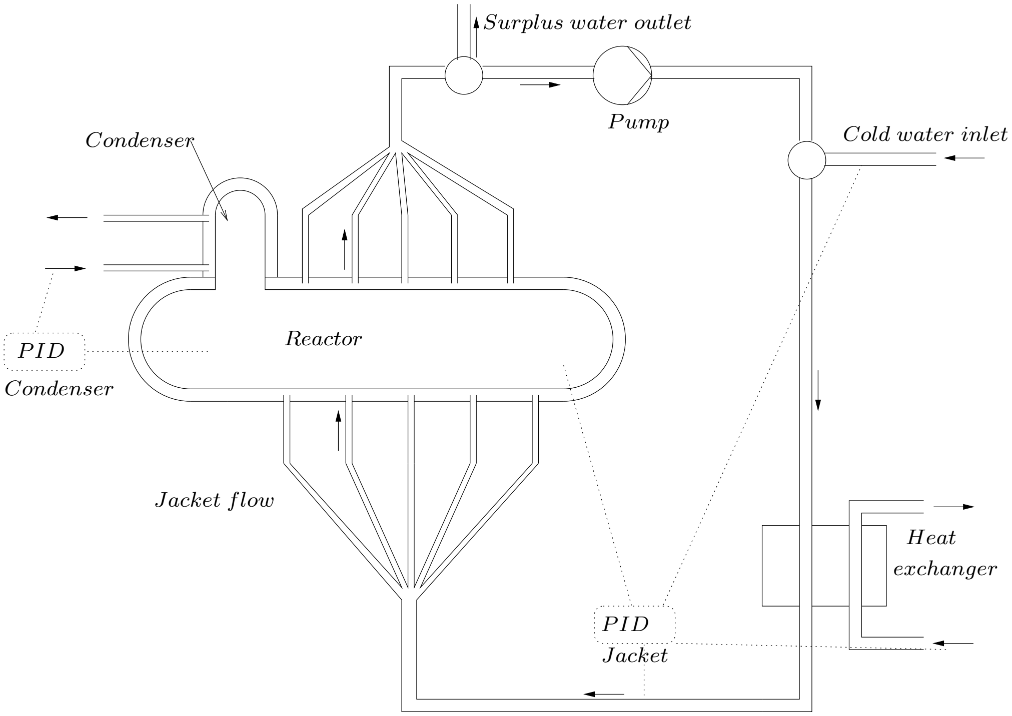

Figure 9: The control system of the process includes two PID controllers. The jacket PID controller consists of a 'master and slave system' and controls the inlet temperature and the heat exchanger.

3.3.1 PID Controller

In the process, sampled versions of a PID controller are used in controlling the jacket temperature and the condenser flow. The control algorithm, with the set point value r, controlled variable y and control variable u, is

$$u = K\left(\beta r - y + \frac{1}{T_I}\int (r-y)\,dt - T_D\frac{dy}{dt}\right). \tag{23}$$

The set point factor β is a constant that is rarely used in this process (that is, it is usually set to 1), unless the auto-tuning program in the system sets it. The inclusion of the factor β allows the loop to be made faster without causing big overshoots at set point changes. In Equation (23), all variables are expressed in percents. The units of the parameters T_I and T_D are given in seconds, which also is the unit for the integration and the derivation in the formula.

In the condenser, $u = F_{Cond}/F_{Cond,Max}$, and $y = P_{Reactor}/P_{Max}$, and in the jacket $u = T_{Jacket}/T_0$ and $y = T_{Reactor}/T_0$, where T_0 is a reference temperature; here we use $T_0 = T_{reactor,Max}$.

In the process, the gains K, T_I, and T_D of the PID controllers vary over time as shown in Figure 10. In this first model, due to limited time, we use constant gains, which results in some errors, see Section 3.6.

3.3.2 Jacket

An advanced control system, consisting of 'master and slaves' controllers, controls the jacket input temperature, involving a steam heat exchanger and a raw (cold) water inlet. PID controllers are used for both the heat exchanger and the raw water inlet. In this first model, we implement only one PID controller, the master controller and use the technical limits from the heat exchanger and the raw water mixing as constraints on the jacket flow. This approximation results in errors, but these errors are small enough to allow us to consider that the approximation captures the most important physical aspects of the process, such that the model can be used for optimization, see Section 3.6. In future models, the other PID controllers should also be regarded. These constraints concern maximal allowed changes in the jacket temperature (temperature derivatives), as well as limits on the temperature:

$$m \le \frac{\partial T_{jacket}}{\partial t} \le M, \tag{24a}$$

$$c \le T_{jacket} \le C. \tag{24b}$$

3.3.3 Condenser

Generally, pressure reacts very fast to changes in a state of the system, and therefore heat transfer due to condensation is very effective.

Here, the condenser is used only for cooling, and hence, during the heating sequences of the batch only the jacket is used. The condenser system is controlled by

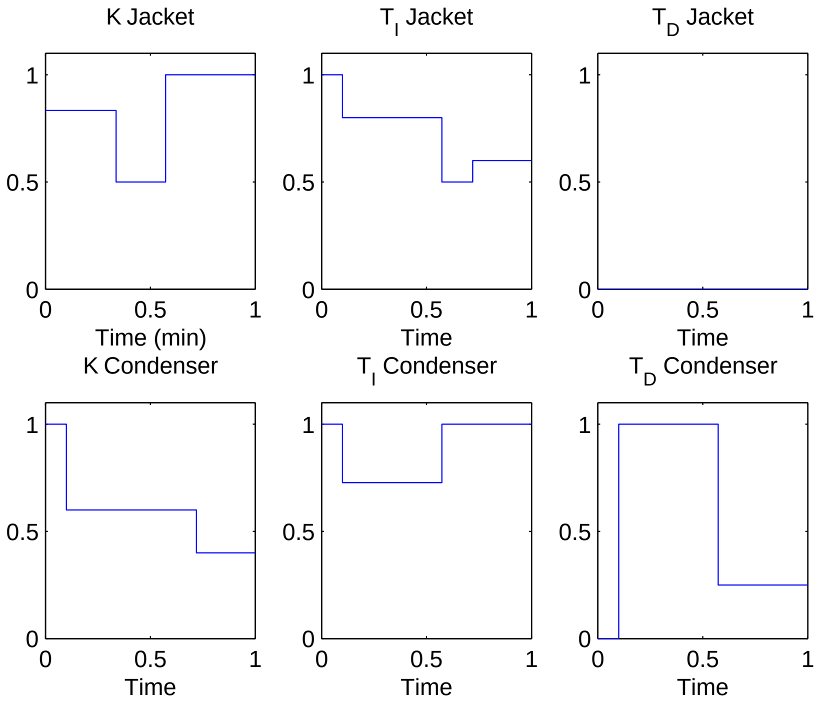

Figure 10: In the real process, the gains of the controllers vary over time. For the jacket, the scaled 'master' PID controller is shown in the upper three graphs. In our model we use constant gains.

the pressure in the reactor; moreover, the condenser functions as a safety control: if the reactor pressure changes too fast the condenser flow starts until the temperature increase has diminished.

As above we use technical limits on the flow as constraints on the condenser flow. These constraints concern maximal allowed changes (derivatives) in the flow, as well as limits on the maximal and minimal flow:

$$l \leq \frac{\partial F_{cond}}{\partial t} \leq L, \tag{25a}$$

$$0 \leq F_{cond} \leq D. \tag{25b}$$

3.3.4 Set point curves

At this stage the set point curves are implemented as functions of the EO addition. The set point temperature T_{set} and the set point pressure P_{set} are raised from the initial set point curves simultaneous with the start of the addition of EO. The slopes are given before-hand for both set point curves and are not affected by the optimization at this stage, but could very well be optimized in the future. Also the second set point raise is determined to start at the end time of the EO addition, see Figure 11.

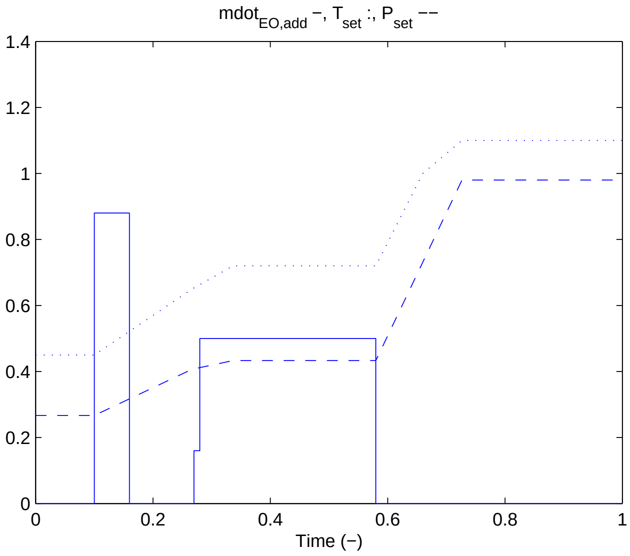

Figure 11: Construction of the set point curves T_{set} and P_{set} from the EO addition curve.

3.4 Pressure

Reactor pressure is used in the condenser controller as the controlled variable y in Equation (23), and therefore we need an expression for this variable.

As a first try, the pressure is obtained assuming an ideal gas where the free gas volume is the volume of the reactor reduced by the volume of cellulose and the volume of NaOH(aq):

$$P^{EK}_{ideal} = \frac{n_{EC}RT}{V_{reactor} - V_{NaOH(aq)-V_{Cellulose}}}. \tag{26}$$

We use values for the specific volume of pulp fibres ($0.62\ 10^{-3}\ m^3/kg$), the density of NaOH(aq) (taken from [27]) and assume no extra effects in volume in alkalization, Reaction (4). At higher temperatures, this calculated pressure is about $33\ \%$ too low compared to the measured reactor temperature, which can be seen in Figure 12. It should be mentioned that the model behind the figure contains no PID controller, but a preset flow through the condenser is used. To get a better pressure model, resulting in Equation (27a), we perform a deeper analysis of the vapor–liquid equilibrium in the reactor, which now follows.

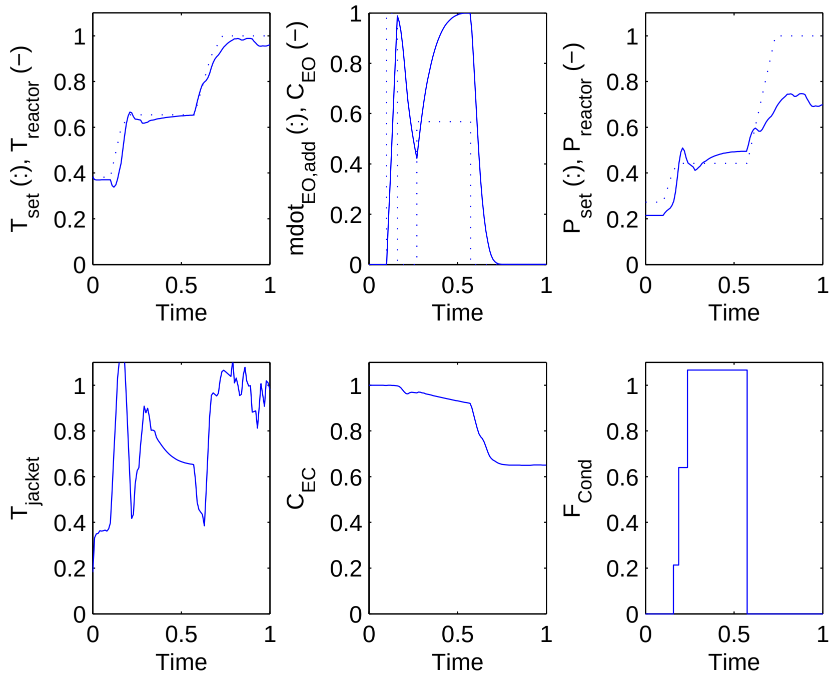

Figure 12: Results from MATLAB using the ideal gas law to calculate pressure, and no controller for the condenser.

After loading the ground cellulose (a very fine powder), the reactor is evacuated to about $5\ kPa$. This amount of gas is neglected in the calculations, since most of the gases are inert.

After the addition of NaOH(aq), EC is added. The amount is larger than the corresponding vapor pressure, which is why part of the EC must be in liquid form. In laboratory trials at Akzo Nobel, it has been seen that an amount about three times larger than used in the process is needed to be able to visually recognize any liquid (at normal pressure) in the cellulose. Hence, a large part of the liquid EC must be absorbed in the cellulose particles. This probably affects the vapor–liquid equilibrium. Observe that EC and NaOH alone are immiscible. This change in the amount of EC available for pressure build up is assumed to be linear in the amount of EC molecules in the reactor. The effect is assumed present also when modeling the EO pressure, see Equation (27b).

In the alkalization process, the structures of the crystalline areas of cellulose are expanded, allowing the hydroxyl groups to be transformed into alcoholate, see Figure 15, which increases the number of polar groups in the cellulose chain. We suggest that this expansion makes it possible to increase the absorption of EC, which is a polar molecule, whereby the vapor–liquid equilibrium of EC is affected. As the EO reaction progresses EO molecules add to the cellulose chain reacting with the alcoholate ions, forcing the chains further apart; see Figures 16 and 17 below. We assume also this expansion to affect the vapor-liquid equilibrium of EC linearly in the progress of the EO-reaction.

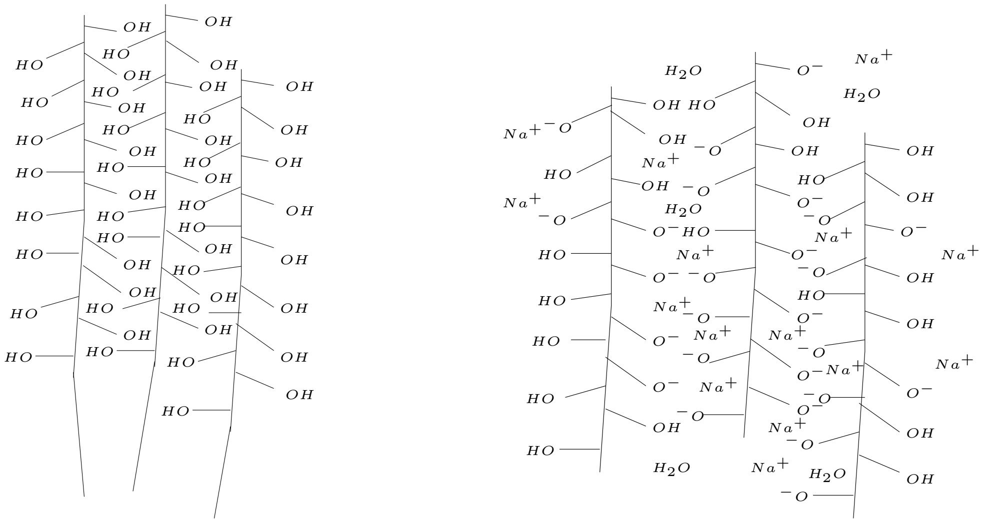

a b

Figure 15: When cellulose (a) is treated with NaOH the crystalline areas are expanded, resulting in alkali cellulose (b).

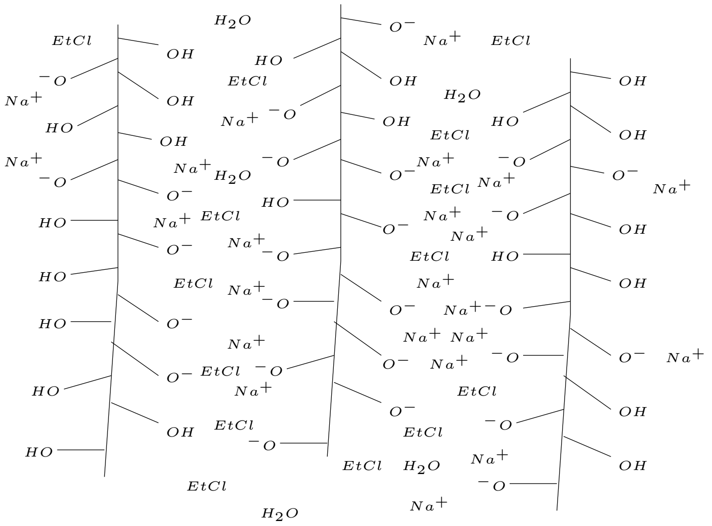

Figure 16: During the EO-reaction, the cellulose chains are forced further apart (compare with Figures 15 and 17), thereby increasing the ability to absorb EC molecules.

Hence, the pressure is modeled in the following way:

$$P_{Reactor} = P_{EO} + P_{EC}, \tag{27a}$$

$$P_{EO} = P^o_{EO}(T)(\alpha_1 n_{EO} + \beta_1), \tag{27b}$$

$$P_{EC} = P^o_{EC}(T)(\alpha_2 n_{EC} + \beta_2)(\gamma_1 \lambda_{EO} + \delta_1), \tag{27c}$$

where P^o_i is the vapor pressure for species i, with values of the constants given in Table 3, on the form

$$P^o_i = 10^{(A + \frac{B}{T+C})}. \tag{28}$$

Table 3: Constants used in Equation (28) for vapor pressure. (Temperature is given in Kelvin and pressure in mmHg; 1 mm Hg = 133.322368 Pa.)

	A	B	C
EO	7.26969	−1114.78	−29.849
EC	7.13047	−1097.60	−27.141

In Equation (27c), the function $\lambda_{EO}(t) \in [0,1]$ describes the progress of the EO-reaction:

$$\lambda_{EO}(t) = \frac{n_{EO,reacted}(t)}{n^{max}_{EO,reacted}}. \tag{29}$$

The variables n_{EC} and n_{EO} in Equation (27) describe the number of moles of EC and EO, respectively, in the reactor, and are given by mass balances for substance

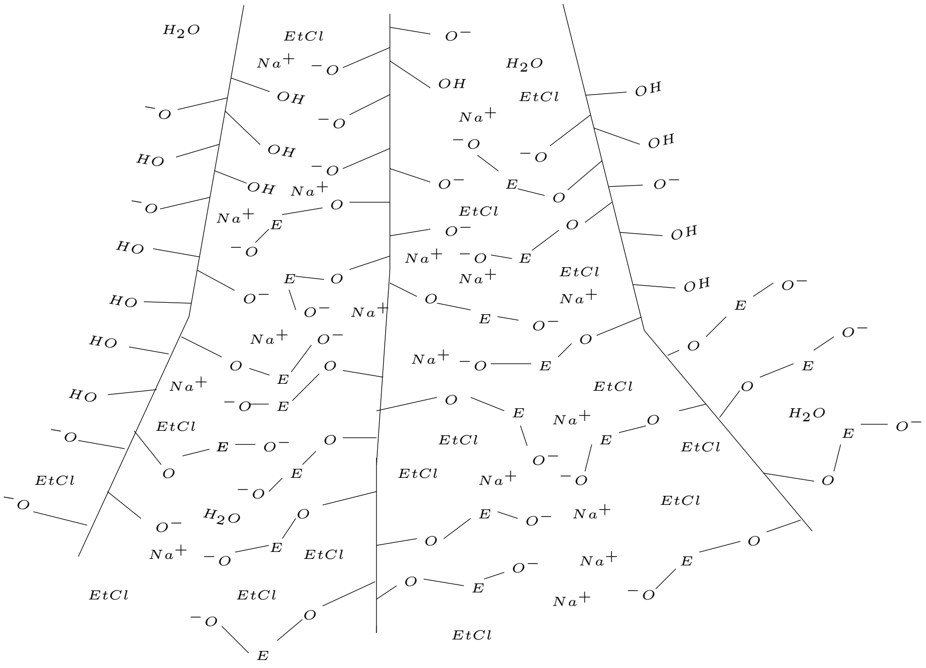

Figure 17: At the end of the EO-reaction the cellulose chains are far apart, compared to in Figure 16, and the ability to absorb EC molecules is high.

$i = EO, EC$:

$$n_i(t) = n_{i,loaded}(t) - n_{i,reacted}(t) = \frac{m_{i,loaded}(t)}{M_i} - \int_0^t r_i \frac{m_{cell}}{M_{AGU}}\, dt. \tag{30}$$

Since EO contributes to the pressure only when present in the reactor, $\beta_1 = 0$ and $\gamma_1 = 0$ hold in Equation (27). The constants α_2 and β_2 are obtained by linear regression, using data from times when only EC is present in the reactor, that is, before EO is added. When this is made, the constants α_1 and δ_1 are obtained by linear regression, using data from several batches and the whole batch duration.

In order to fully describe the system and to calculate the pressure in the reactor, mass balances for the involved substances are needed:

$$\frac{\partial n_{\mathrm{EO}}}{\partial t} = \dot{n}_{\mathrm{EO\_}add} - \dot{n}_{EO,reacted} = \dot{m}_{\mathrm{EO\_}add}\frac{1}{M_{\mathrm{EO}}} - k_{EO}(T)n_{\mathrm{EO}}, \tag{31a}$$

$$\frac{\partial n_{\mathrm{EC}}}{\partial t} = -r_{EC}\frac{M_{AGU}}{M_{EC}} = -k_{EC}(T)n_{\mathrm{EC}}n_{\mathrm{RO^-}}\frac{M_{NaOH}}{M_{AGU}}, \tag{31b}$$

$$\frac{\partial n_{\mathrm{RO^-}}}{\partial t} = -r_{EC}\frac{M_{AGU}}{M_{NaOH}} = -k_{EC}(T)n_{\mathrm{EC}}n_{\mathrm{RO^-}}\frac{M_{EC}}{M_{AGU}}. \tag{31c}$$

The initial values are given as

$$n_{\mathrm{EO}}(0) = 0, \tag{32a}$$

$$n_{\mathrm{EC}}(0) = c_{EC,0}\frac{M_{AGU}}{M_{EC}}, \tag{32b}$$

$$n_{\mathrm{RO}^-}(0) = c_{RO^-,0}\frac{M_{AGU}}{M_{NaOH}} = c_{\mathrm{NaOH},0}\frac{M_{AGU}}{M_{NaOH}}. \tag{32c}$$

Summing up, the pressure is modeled using physical aspects at the molecular level and depend on the reactor temperature, the amount of EO and EC in the reactor, as well as on the progress of one of the involved reactions. The mathematical description is given by Equations (27)–(32).

3.5 Parameter Estimation

Data from ten batches has been used to estimate parameters. Process data has been available for every minute; see Table 4 for a list of data used.

Table 4: Data available

Description	Variable	Unit
Time	t	min
Reactor pressure	P	kPa
Reactor temperature	T_r	K or °C
Loaded NaOH	m_{NaOH}	kg
Loaded EO	$m_{EO,\ add}$	kg
Loaded EC	m_{EC}	kg
Flow jacket	F_{jacket}	m3/h
Temperature in, jacket	$T_{jacket,in}$	K
Temperature out, jacket	$T_{jacket,out}$	K
Flow condenser	F_{cond}	m3/h
Temperature out, condenser	$T_{cond,out}$	K
Temperature in, condenser = temperature, cold water	$T_{cond,in}$	K

3.5.1 Estimation of concentrations

The concentrations can not be measured in the reactor, but an estimation of the concentrations, c_i, and the reaction rates, r_i, has been made by Akzo Nobel prior to this study, using a discretization of Equation (21). Assuming that nothing is added or removed during a time step $\Delta_j = [t_{j-1}, t_j]$, the discretization gives the following:

$$c_{\mathrm{EO}}(t_j) = c_{\mathrm{EO}}(t_{j-1})e^{-k_{EO}(t_j)}, \tag{33a}$$

$$c_{\mathrm{EC}}(t_j) = \frac{(c_{\mathrm{EC}}(t_{j-1}) - c_{\mathrm{RO}^-}(t_{j-1})c_{\mathrm{EC}}(t_{j-1})}{c_{\mathrm{EC}}(t_{j-1}) - c_{\mathrm{RO}^-}(t_{j-1})e^{k_{EC}(t_j)(c_{\mathrm{RO}^-}(t_{j-1})-c_{\mathrm{EC}}(t_{j-1}))t_j}}, \tag{33b}$$

$$c_{\mathrm{RO}^-}(t_j) = \frac{(c_{\mathrm{RO}^-}(t_{j-1}) - c_{\mathrm{EC}}(t_{j-1}))c_{\mathrm{RO}^-}(t_{j-1})}{c_{\mathrm{RO}^-}(t_{j-1}) - c_{\mathrm{EC}}(t_{j-1})e^{k_{EC(t_j)}(c_{\mathrm{EC}(t_{j-1})}-c_{\mathrm{RO}^-}(t_{j-1}))t_j}}. \tag{33c}$$

Here we assume that the addition of EO is made instantly at the discretization times t_{j-1}, that is $c_{\mathrm{EO}}(t_{j-1})$ includes added EO during the last time interval Δ_{j-1}.

These equations are used together with process data (the reactor temperature) to calculate the concentrations, when comparing the mathematical model to the real process data in Figure 7.

3.5.2 Estimation of reactor pressure

When estimating the reactor pressure, P_r, data from three different batches has been used. The number of moles of substance i, $i = EO,\ EC$ present in the reactor, $n_i(t_j)$, are calculated at each time step using Equations (33) and the measured reactor pressures P_j and temperatures T_j.

3.5.3 Estimation of heat transfer coefficients

To estimate k_{jacket}, the heat transfer coefficient of the jacket, we state equations for the heat flow over the jacket and from the reactor to the jacket:

$$Q = F_w C_{P,w}(T_{out} - T_{in}),$$
$$Q = kA_r(T_{jacket} - T_{reactor}),$$

where the reactor area is known to be approximately $A_r = 20\ m^2$. The flow through the reactor is high enough, $F_w = 100\ m^3/h$, and the temperature difference between inflow temperature and outflow temperature is less than $5K$ (compared to $50K$ over one batch), to approximate the jacket temperature as the out temperature. A heat balance assuming no accumulation term gives

$$Q = kA_r(T_{out} - T_r),$$

which implies that

$$k = \frac{F_w C_{P,w}(T_{out} - T_{in})}{A_r(T_{out} - T_r)}.$$

This estimation of k has been tabulated; Figure 18 shows an example of one batch. As can be seen, the k_{jacket} is not constant as expected, and one reason can be that the calculation is made without taking into account any delays (no accumulation term): in the derivation of k we assumed that Q is constant, which is not the case. The addition of 'cold' EO ($T_{add} < T_r$) involve a cooling of the reactor content as well as

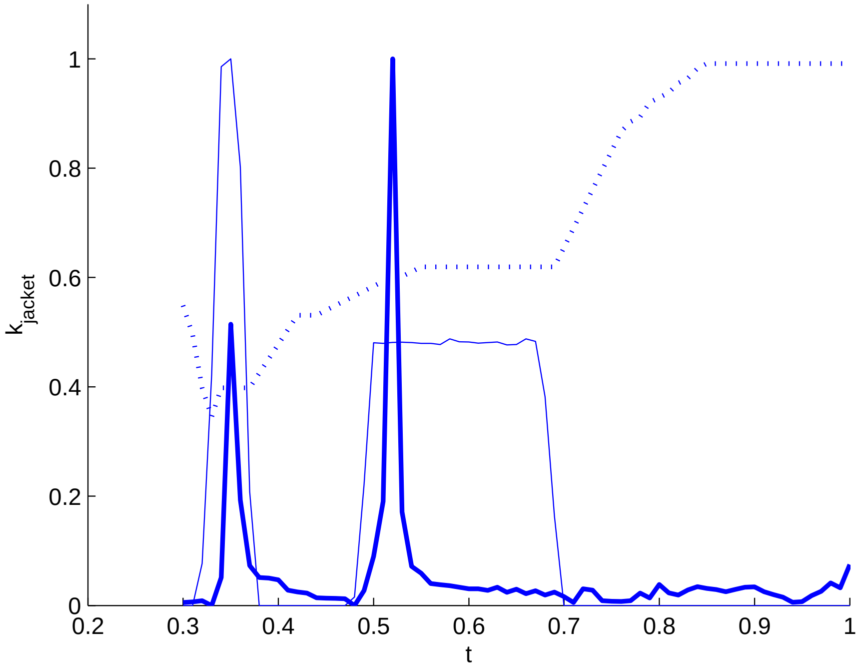

Figure 18: The bolded graph shows the estimation of k_{jacket} at different times. The set temperature T_{set} (dotted graph) and the EO addition $\dot{m}_{EO}$ (thin graph) is also shown.

a vaporization of the liquid EO to gaseous EO, which requires energy. Both these actions change the reactor temperature faster than what can be detected from data available, which in Figure 18 is seen in that k is not constant. Data from times where no EO is added and the condenser is not used ha been used to calculate an average from three batches.

The value of heat transfer coefficient k for the condenser is estimated likewise; see Figure 19. The coefficient is available only during those parts of the batch where the condenser is used. As can be seen, nor k_{cond} is constant during the batch. As for the jacket, one reason can be that the calculation is made without taking into account any delays. When the condenser is used, heat is withdrawn both through the jacket and the condenser at the same time, and in addition EO is added (with the effects discussed above), which makes the estimation even less accurate. To model the heat transfer coefficients with higher accuracy, more data is needed, as well as additional experiments. At this stage this is what we use, but it would be interesting to study this more thoroughly.

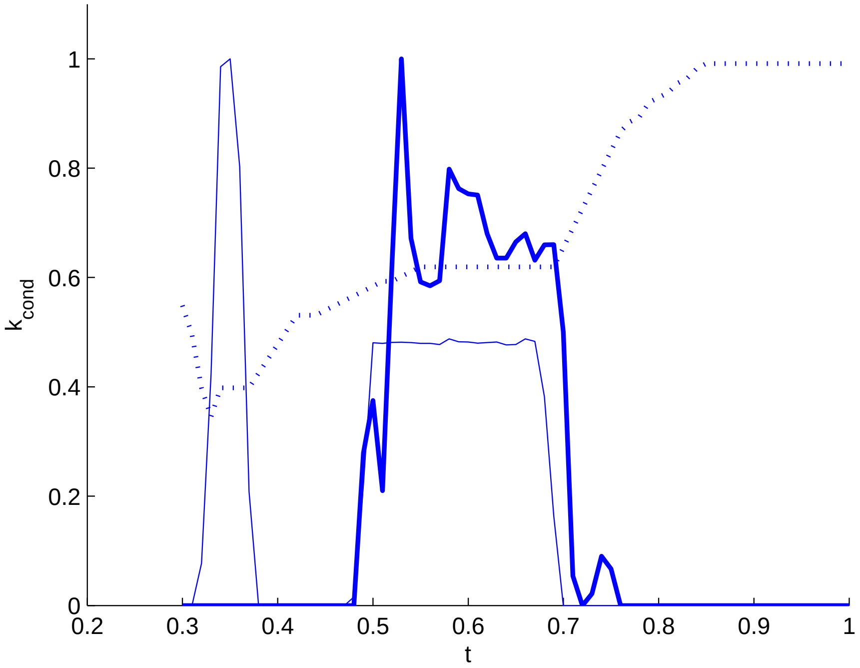

Figure 19: The bold graph shows the estimation of k_{cond} at times when the condenser is used. The set temperature T_{set} (dotted graph) and the EO addition $\dot{m}_{EO}$ (thin graph) is also shown.

3.6 Simulation results and discussion

The mathematical description of the batch reactor used in this work is given by the equations in Sections 3.2–3.4. These equations have been implemented in SIMULINK, a software package in MATLAB. In the figures below showing simulations, 0.1 time units have been added prior to the starting time for EO addition, to make the figures easier to read. Data has been compared to real process data by converting the EXCEL files (with process data) from Akzo Nobel to MATLAB.

In SIMULINK a PID controller is described by a differential equation,

$$\begin{aligned} u(t) &= u_p(t) + u_i(t) + u_d(t) \\ &= Ke(t) + \frac{K}{T_i}\int_0^t e(t)\,dt + KT_d\frac{de(t)}{dt}, \end{aligned}$$

where the output u is the sum of a proportional term u_p, an integral term u_i, and a derivative term u_d, cf. Equation (23), K is the proportional gain of the PID controller, $e(t)$ is the error between the reference and feedback inputs, and T_d is the derivative time of the controller.

In discrete terms the derivative gain is defined as $K_d = T_d/T$ and the integral gain is defined as $K_i = T/T_i$, where T is the sampling period and T_i is the integral time of the PID controller.

In the mathematical model, not all parameters are known, or the estimated values do not give curves in agreement with real process data when implemented in SIMULINK and MATLAB; compare Figure 20 with Figure 7 on page 16. Trials have been made in SIMULINK to find values of $C_{P,tot}$, ΔH_{EO}, ΔH_{EC}, K_{jacket}, $T_{I,jacket}$, and $T_{D,jacket}$ that make the model agree with the real process data as well as possible. Table 5 shows the estimated and the used model values. We argue that the errors that remain when using the values in Table 5 are small enough to capture the most important physical aspects of the process, such that the model can be used for optimization. Figure 21 shows a simulation with the parameter values as is shown in Table 5. The figure should be compared to a typical real batch, such as Figure 7 on page 16. As can be seen, all simulated curves but the jacket temperature follow the real curves quite well. The simulated jacket temperature rises in the beginning, as does the real jacket temperature, but then, during the time interval of 0.3–0.7 time

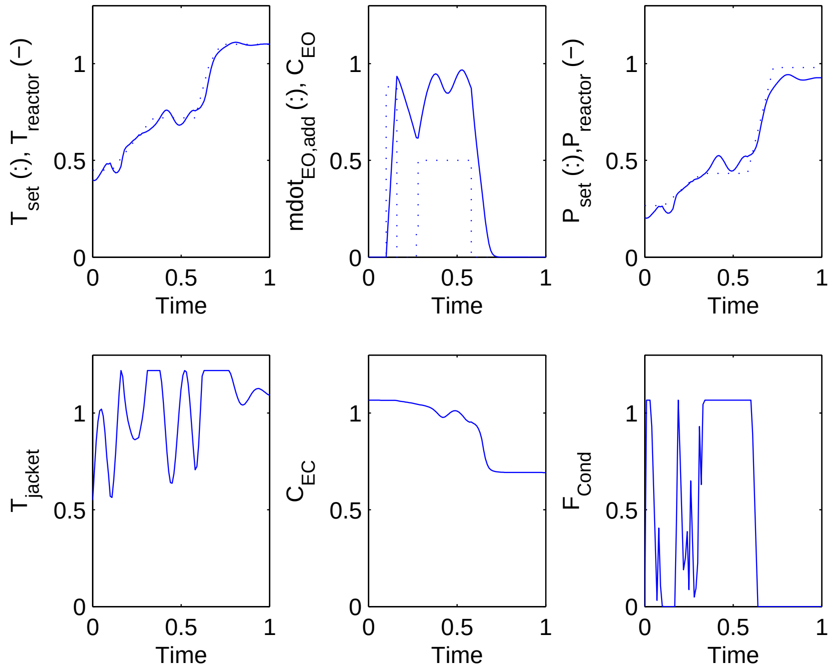

Figure 20: The figure shows a simulation where the PID parameter $T_{I,jacket} = 1.0$ min. As can be seen the jacket temperature T_j does not follow the real jacket temperature in Figure 7 on page 16.

Table 5: Comparison between estimated values and values that makes the mathematical model agree with the real process data.

Constant	**Estimated value**	**Value used in SIMULINK**
$C_{P,tot}$ $(kJ/mole, K)$	6	5.5
ΔH_{EO} $(kJ/mole)$	150	150
ΔH_{EC} $(kJ/mole)$	(small)	0
k_{jacket} $(W/m^2, K)$	700	900
k_{cond} $(W/m^2, K)$	500	600
K_{jacket} (–)	3.00	3.00
$T_{I,jacket}$ (min)	1–1.33	0.10
$T_{D,jacket}$ (min)	0	0

units, it does not fall far enough compared to the real jacket temperature. This error, in turn, affects all the other variables in this time interval: the simulated reactor temperature is somewhat lower than the real one, the simulated pressure is somewhat higher than the real one, and there are twitches in the simulated concentrations c_{EO} and c_{EC} which are not present in the real concentrations. This error is possibly due to two major things: first, in the simulations we use constant PID parameter values instead of time variable ones, and second, the heat transfer between the reactor content and the jacket water is modeled with rather low accuracy, see Section 3.5.3. In this work, the focus has been on making a simple model to use as a start for further modeling work, and this is why we have chosen to use these approximated values. The relation between the effects of the approximations is difficult to say anything about without further information. In the future, these things should be looked further into.

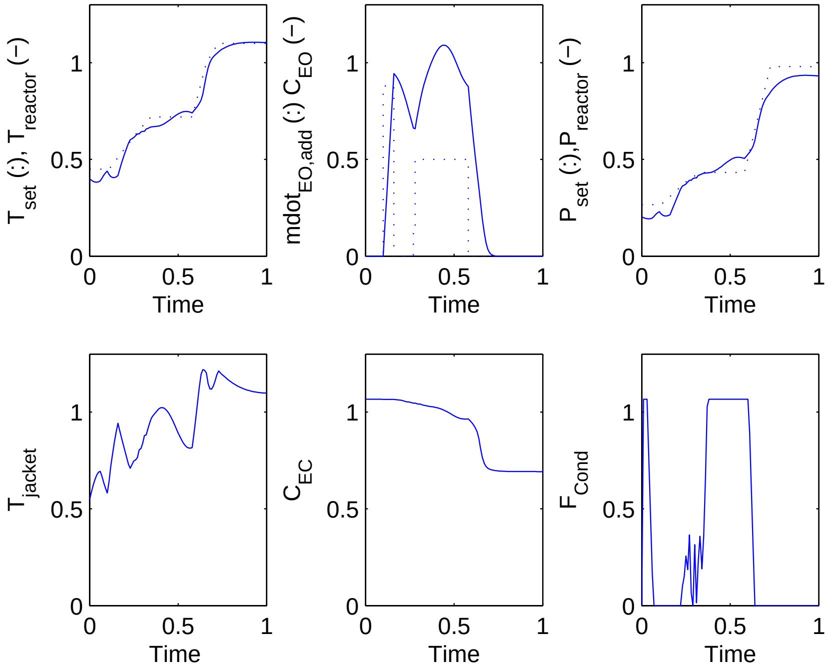

Figure 21: A simulation in SIMULINK with parameter values given in Table 5.

4 Optimization and analysis

4.1 Formulation as an optimization problem

We want to minimize the total batch time and hence use the complete model in Section 3 to formulate the dynamic minimum time problem, Equation (3). It has the form

$$\begin{aligned}
&\text{minimize} && t_f, && \text{(34a)}\\[1ex]
&\text{subject to} && h(\dot{x}(t), x(t), u(t), t) = 0, && \text{(34b)}\\
& && g(x(t), u(t), t) \leq 0, && \text{(34c)}\\
& && x \in X, u(t) \in U, && \text{(34d)}\\
& && x(0) \in X_0, x(t_f) \in X_f, && \text{(34e)}\\
& && t \geq 0. && \text{(34f)}
\end{aligned}$$

In this formulation, the system equations h are given by the model in Section 3, including the constraints.

The overall heat balance, given by Equations (9)–(22), can be summarized by

$$\dot{T}_r = f_1(T_r, n_{EO}, n_{EC}, n_{RO^-}, T_j, F_{cond}, t, \dot{m}_{EO,add}), \tag{35}$$

since $n_i = c_i \frac{m_{Cell,0}}{M_{AGU}}$; the PID controllers for the jacket and the condenser, Equation (23), can be rewritten as

$$\begin{aligned}
\dot{T}_j &= f_2(T_r, n_{EO}, n_{EC}, n_{RO^-}, T_j, F_{cond}, t, \dot{m}_{EO,add}), && \text{(36)}\\
\dot{F}_{cond} &= f_3(T_r, n_{EO}, n_{EC}, n_{RO^-}, t, \dot{m}_{EO,add}). && \text{(37)}
\end{aligned}$$

The reactor pressure is described mathematically by Equations (27a)–(32), and these equations can be summarized as

$$\begin{aligned}
\dot{n}_{EO} &= f_4(T_r, n_{EO}, t, \dot{m}_{EO,add}), && \text{(38)}\\
\dot{n}_{EC} &= f_5(T_r, n_{EC}, n_{RO^-}, t), && \text{(39)}\\
\dot{n}_{RO^-} &= f_6(T_r, n_{EC}, n_{RO^-}, t). && \text{(40)}
\end{aligned}$$

In these equations, all variables T_r, n_{EO}, n_{EC}, n_{RO^-}, T_j, F_{cond}, $\dot{m}_{EO,add}$ are functions of the time t. Initial values are known and are included in the description of X_0 in Equation (34) for all these equations.

Additional constraints, natural [(34d) and (34e)] or given from the process [(34c)] as discussed in the modeling section, are that

$$\begin{aligned}
0 \leq{} & T_r, && && \text{(41a)}\\
c \leq{} & T_j && \leq C, && \text{(41b)}\\
m \leq{} & \frac{\partial T_j}{\partial t} && \leq M, && \text{(41c)}\\
0 \leq{} & F_{cond} && \leq D, && \text{(41d)}\\
l \leq{} & \frac{\partial F_{cond}}{\partial t} && \leq L, && \text{(41e)}
\end{aligned}$$

$$\begin{aligned} 0 \leq \quad n_{EO} \quad &\leq n_{EO,max}, && \text{(41f)}\\ 0 \leq \quad n_{EC} \quad &\leq n_{EC,max}, && \text{(41g)}\\ 0 \leq \quad n_{RO^-} \quad &\leq n_{RO^-,max}. && \text{(41h)} \end{aligned}$$

We want to minimize the total batch time for the process, which from the process manager's point of view is from loading to emptying the reactor. In this study, we consider the reactions starting with the addition of ethylene oxide, including the heat transfer from the reactor, but not loading, preheating, cooling and emptying. We define the end of the batch as the time t_f characterized by the concentration of EC dropping below a limit c^0_{EC}. We optimize the operation by finding an optimal way of adding the ethylene oxide to the reactor ($\dot{m}_{EO,\,add}(t)$). This can mathematically be written as, cf. Equation (3):

$$\begin{aligned} \text{minimize} \quad & t_f, && \text{(42a)}\\[6pt] \text{subject to} \quad & h(\dot{x}(t), x(t), u(t), t) = 0, && \text{(42b)}\\ & g(x(t), u(t), t) \leq 0, && \text{(42c)}\\ & x \in X,\ u(t) \in U, && \text{(42d)}\\ & x(0) \in X_0,\ x(t_f) \in X_f, && \text{(42e)}\\ & t \geq 0, && \text{(42f)} \end{aligned}$$

where $x^\top = (T_r, T_j, F_{cond}, n_{EO}, n_{EC}, n_{RO^-})$, the differential algebraic equations (42b) are given by Equations (35)–(40) (including initial values $x(0) \in X_0$), and the constraints (42c) are given by Equations (41).

The optimal control vector profile u, which in this case is the function $\dot{m}_{EO,add}(t)$, can be determined by using a control vector parametrization approach for the solution of the dynamic optimization problem. This means that the optimization is performed on two levels, one level where the optimization is performed, and one level where the DAE is solved, see Figure 3.

4.2 Manual optimization

To gain information about our system and at the same time improving the batch time, a manual optimization is performed, using SIMULINK, MATLAB. Below, we describe the details of this optimization.

The function $\dot{m}_{EO,add}(t)$ is parameterized by dividing the batch time into $J = 150$ equal time elements and assuming the flow rate to be constant in each of these elements. To prevent too fast changes in flow rate (which originates from limited capability of pumps etc.), two adjacent elements are not allowed to differ more than a preset value, α:

$$\begin{aligned} \dot{m}_{EO,add}(t) = m_j, &\quad t \in [t_{j-1}, t_j),\ j = 1, \ldots, J\\ |m_j - m_{j-1}| \leq \alpha, &\quad j = 2, \ldots, J. \end{aligned}$$

To prevent too high temperatures and too large temperature gradients, which are not allowed in the real process, but is accepted by MATLAB in simulations, a penalty is added to the objective function:

$$f_{obj} = t_f + P. \tag{43}$$

As a first step, used in the simulations below, a discontinuous penalty is used, namely

$$P(T_r) = \begin{cases} p, & |T_{set} - T_r| \geq \beta, \\ 0, & \text{otherwise}, \end{cases} \tag{44}$$

where $p \gg 0$. It should be mentioned that when performing an automatic optimization, a continuous penalty is preferred, for instance the following

$$P(T_r) = p \max\{0, |T_{set} - T_r| - \beta\}. \tag{45}$$

The penalty P is added in those simulations where the control system does not manage to keep the reactor temperature close enough to the set point temperature T_{set}. The constant β is determined by the ability of the PID controllers to control the reactor temperature and a large value means that the jacket is good at controlling the reactor temperature. Since a DAE system is just a model of the real system, it contains errors, and the constant β is also used as an additional error control of the reactor heat transfer and the control system. If the error in the control system and/or the reactor heat transfer is large and the simulated system is able to control the reactor temperature, a small value of the constant β in Equations (44) and (45) decreases the risk of escalating reactor temperature in the real reactor.

In this study, the focus has been on finding a mathematical model for the batch time, and initially not on the quality of the end product. Still, we need to use information about the end product quality to determine which profiles are acceptable: if a large portion of the EO is added prior to the wanted reaction temperature is reached, this may result in a worsened product quality. Below, this is judged by the user. Since, prior to this study, there is a lack of knowledge about how the quality is affected by different temperature profiles, adding this to the mathematical model would have been to comprehensive. The acceptable size of the portion of EO added prior to the wanted reaction temperature and how the quality is affected by the reaction temperature are interesting future research topics. To get a proper objective function, the quality should be added to the optimization problem, for instance as a penalty in the objective function just as large temperature gradients above.

Below we use the objective function defined by Equation (43), including a discontinuous penalty according to Equation (44) with $p = 10$. This means that an objective function value above 10 has been penalized. For the original EO profile in Figure 21, this objective function value is $f_{obj} = 0.61$.

In each step in the manual optimization, we change as little as possible, to clearly notice the effects. We compare each simulation with the original profile used in the process today. All simulations have in common that the slopes and the plateau values of the set point curves T_{set} and P_{set} (see Section 3.3.4 for definitions) are the same as in the original profile. The starting time for the second set point rise is determined by the end of the EO addition. A reason for not allowing changes in slopes for the set point curves, is that if the reactor temperature (or pressure) rises too fast, there is a potential risk for escalating reactor temperature, which is not wanted; it is even dangerous. Of course, varying the set point curves would be interesting to include in a future optimization. The different profiles are tested according to the following scheme.

1. To start with, we fix the starting time of the EO addition to equal the start of the first set point rise.
    (a) We test some basic profiles, which are small variations of the original.
    (b) Using the shape of the original profile with two plateaus with different levels, we investigate how the levels of the plateaus affect the batch time:
        - keeping the first plateau level as the original, varying only the second plateau,
        - varying both plateau levels proportionally; and
        - varying both plateau levels separately. Only a small number of profiles have been tested — a more thorough investigation of trial profiles is recommended.
2. We relax the starting times for the rise of the set point curves by delaying the start of the EO addition.
    (a) The levels of the plateaus are constant, while the delay is varied.
        - Using the original profile.
        - Using a profile with three plateaus.
    (b) Both the plateau levels and the delay are varied.
        - Using a profile with one plateau.
        - Using the original profile with two plateaus.

4.3 Results and discussion

Several simulations have been run manually, with various EO addition profiles according to the scheme above. The result is shown and discussed here.

1. The start of the EO addition is fixed to the starting time for the first set point rise.
    (a) From the beginning we know that some of the tested basic profiles are not wanted, since they result in a worsened end product quality according to the discussion above. Still, we gain information from these simulations. In most of these simulations, which are found in Appendix A, the plateau levels are the same as the original profile. All we can conclude from these simulations is that a piecewise constant function profile with two or three descending levels tends to result in a short batch time.

(b) Using a profile with two plateau levels as the original and varying only the second plateau level, the second plateau level is possible to raise up to 70 % higher than the original one without an added penalty in the objective function due to control system limitations: levels above 70 % higher than the original is penalized. A 50 % higher level gives the batch time 0.61, which is the same as the original. A 30 % higher level results in a batch time of 0.59, which is an improvement compared to the original.

The batch times for simulations in which the two plateau levels are varied proportionally, are shown in Table 8, with the delay = 0.00. As can be seen, using for instance a 20 % rise in the plateau levels, it is possible to shorten the batch time to 0.58 time units, which is an improvement of 5 % compared to the original profile. According to these simulations nothing is gained by raising the levels further.

An example of simulations where the two plateau levels have been varied separately is shown in Figure 22. The profile that resembles the original profile, but both plateaus have higher levels (14% and 20 %, respectively). The resulting objective function value is 0.58, also 5% better than the original one. As mentioned above, more trials are recommended varying the two plateau levels separately.

2. Relaxing the starting time for the rise of the set point curves by delaying the start of the EO addition, we have performed several simulations, shown below.

   (a) Two series of simulations have been performed in which only the delay is varied, one using the original EO profile and one using the same profile as in Figure 23 with three levels; see Table 6. We conclude that the batch time increases when delaying the original profile, and that using the profile with three plateaus, it is possible to decrease the batch time, with delays up to 0.05 time units. However, the quality must be taken into account, since a portion of the EO is added prior to the reactor temperature reaches the wanted reaction temperature. To determine whether a delayed profile is actually useful, information about the quality must be known. Figure 24 shows a simulation using the original profile with 0.05 time units delay.

Table 6: Objective function values for different simulations.

Delay (time units)	Profile as original	Profile as in Figure 23
0.00	0.61	0.55
0.05	0.65	0.60
0.10	0.69	0.63
0.15	0.74	0.65
0.20	0.78	0.69

   (b) Combinations of variations in delay and variations in levels using only one plateau is shown in Table 7. It is seen that for those simulations

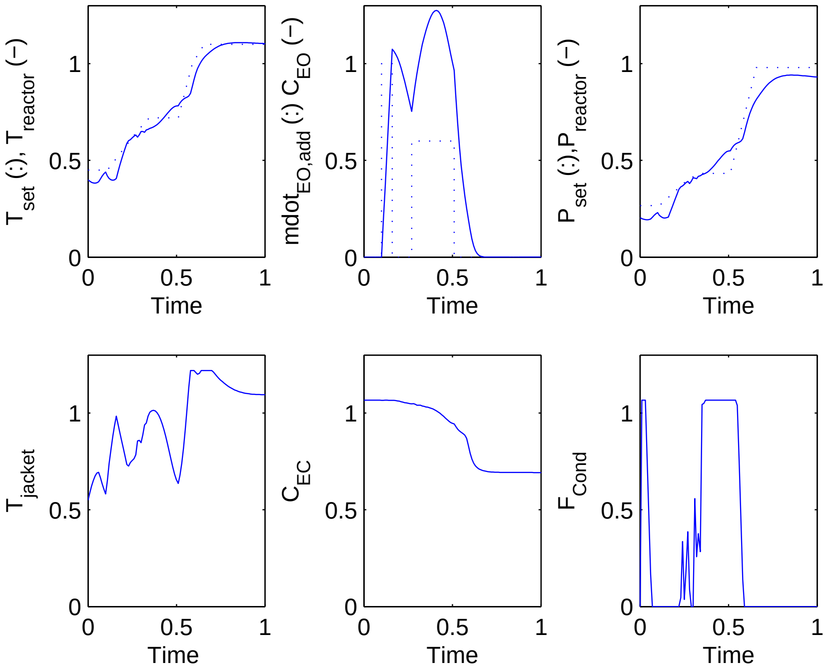

Figure 22: The figure shows a simulation where both the first and the second plateaus have higher levels than in the original profile.

in which the penalty is not activated, the batch time decreases with increasing levels, which is natural since higher concentrations of EO in the reactor results in a higher reaction rate according to Equation (21). But increasing the EO addition too much results in a too large heat production for the control system to handle, which is seen in that the objective function value is penalized and $f_{obj} > 10$. For all level rises, increasing the delay naturally increases the batch time. For the two smallest level rises (1.25 and 1.30) some of the batch times are smaller than the original profile, but one must keep the quality in mind; in order to to determine whether these profiles give acceptable quality, more research is needed.

Combinations of variations in delay and variations in levels using the shape of the original profile is shown in Table 8. In these simulations, the relation between the plateau levels is the same as the original. Here the control system can handle all simulated profiles, but only simulations without delay result in a shorter batch time than the original. As mentioned above, using the original profile without delay the system can handle levels up to 70 % higher than the profile used today without escalating

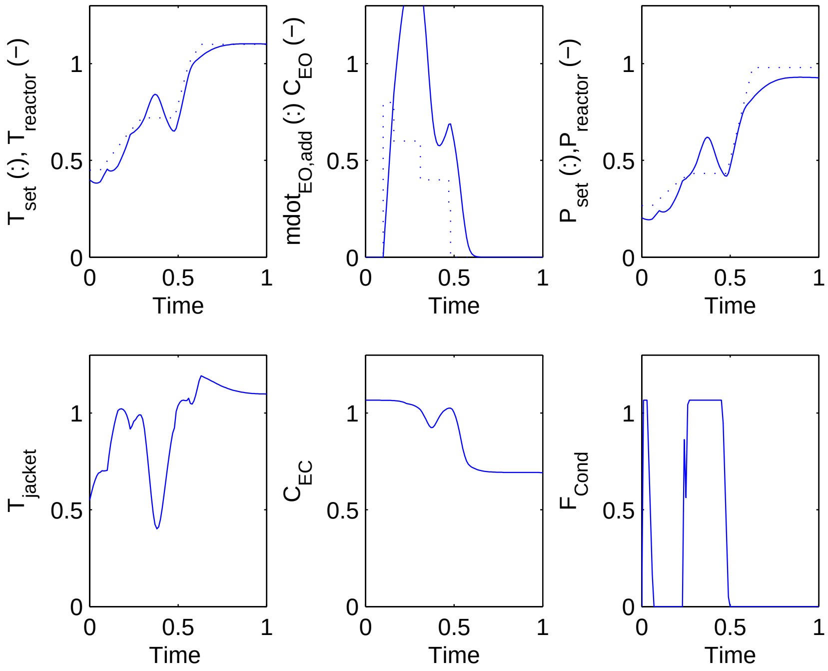

Figure 23: The figure shows a simulation where the EO 'batch plateau' is instantly followed by a second, somewhat lower, plateau level and a third, even lower level. Here the EO addition is delayed 0.05 time units after the set point temperature and pressure risings. The corresponding objective function value is $f_{obj} = 0.60$.

reactor temperatures, with a decrease of 5 % of the original batch time.

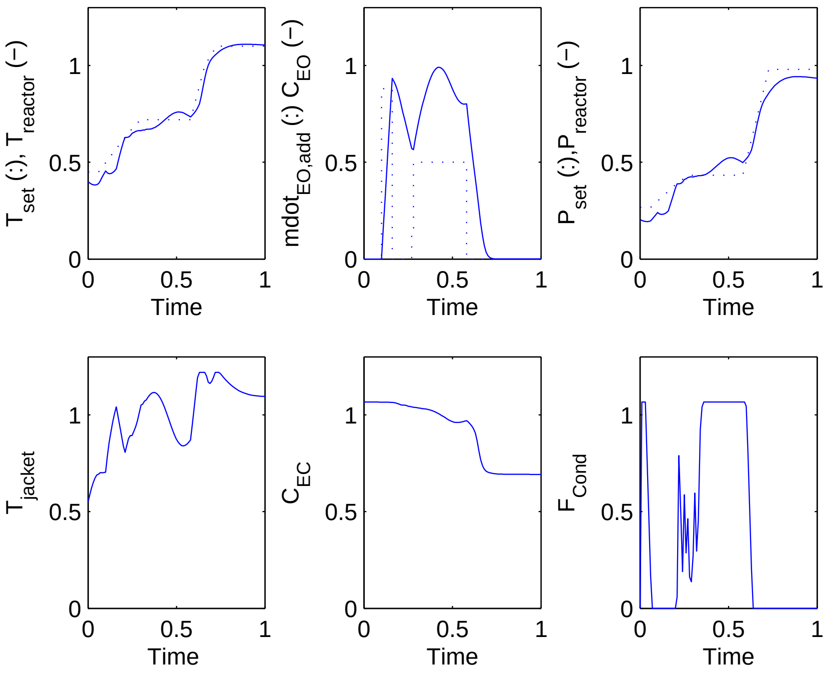

Figure 24: The figure shows a simulation with original EO profile, but where the EO addition is delayed 0.05 time units. The corresponding objective function value is $f_{obj} = 0.65$.

Table 7: Objective function values for different simulations using EO profiles with one single plateau.

	Level rise $l = \frac{New\ levels}{Original\ levels}$				
Delay (time units)	1.25	1.30	1.40	1.50	1.60
0.00	0.57	0.56	10.58	10.55	10.54
0.05	0.60	0.57	10.62	10.58	10.56
0.10	0.63	0.60	10.62	10.62	10.60
0.15	0.67	0.64	0.64	10.65	10.64
0.20	0.71	0.68	0.68	10.69	10.67
0.25	0.76	0.72	0.72	10.73	10.71

Table 8: Objective function values for different simulations, using the shape of the original EO profile but with varying levels and delays.

	Level rise $l = \frac{New\ levels}{Original\ levels}$								
Delay (time units)	1.00	1.10	1.20	1.30	1.40	1.50	1.60	1.70	1.75
0.00	0.61	0.60	0.58	0.58	0.58	0.58	0.58	0.58	10.58
0.05	0.65	0.63	0.62	0.62	0.62	0.61	0.61	0.60	
0.10	0.69	0.68	0.66	0.66	0.66	0.64	0.64	0.62	
0.15	0.74	0.72	0.71	0.71	0.69	0.68	0.68	0.66	
0.20	0.78	0.77	0.75	0.75	0.73	0.72	0.72	0.70	
0.25	0.83	0.81	0.80	0.79	0.78	0.76	0.76	0.74	

5 Conclusions and future work

5.1 Conclusions

In this work we have studied a semi-batch reactor in which EHEC, ethyl hydroxyethyl cellulose, is produced. We have formulated a mathematical model describing the reactor, including the condenser and the jacket. Also the control system has been modeled. The model includes heat and mass balances of the reactor, a pressure model, models of PID controllers and heat and mass balances for the jacket and the condenser. Technical limitations, for instance maximal and minimal jacket temperature changes due to limitations in the heat exchanger, have been modeled as constraints. Uncertainties are not included in the model, but we mention several sources of error in the text.

The system equations have been implemented in SIMULINK, MATLAB and the model predicts the process variables rather well over time. During the EO addition the model is not able to reproduce the jacket temperature to the desired accurateness, but the other variables have acceptable predictions.

The mathematical model has been used to formulate an optimization problem, where the total batch time is to be minimized under the constraints of the differential algebraic equation system and other constraints originating from the process, for instance limited pump capabilities. A manual optimization is performed, in which a discontinuous penalty is used for those simulations where the control system does not manage to keep the reactor temperature close enough to the set point curve. For automatic optimization a continuous penalty should be used instead. The quality of the end product also affects which profiles are acceptable, but it is not known exactly how.

Piecewise constant EO profiles with up to three constant plateaus and varying levels have been used, and simulations show that a 5 % increase in total batch time is possible, using a profile with two plateaus as in the original, but with 20 % higher levels and no delay.

A 10 % shorter batch time than today is possible, using a profile with three different plateau levels. However, in this a profile, a large portion of the EO is added prior to the wanted reaction temperature is reached, which may result in a worsened end product quality. In order to decide which profiles are acceptable, more research about the effect of the reaction temperature used on the end product quality is needed.

It is highly probable that further investigations, and especially automatic optimization, can show profiles resulting in even shorter batch times.

5.2 Future work

Below interesting future research areas, discussed in the main text, are listed, which all aims at decreasing the errors in the model. Which area to prioritize strongly depends on what the model should be used for, and recommendations are therefore difficult to make. The research areas regarding the modeling are listed starting inside the reactor and ending with the control system.

Regarding the modeling, future recommended work includes studies on the phases inside the reactor as well as on the heat transfer between the reactor content and the jacket flow. Different phases inside the reactor give rise to very different behavior and heat transfer. In order to better control the errors regarding the reactor contents and the heat transfer to the wall it is necessary to gain more knowledge about the phases.

Also the condenser, the total jacket system and the control system are interesting to study more thoroughly. In both the jacket and condenser heat transfer, non steady-state balances including heat accumulation in the reactor material are interesting next steps in developing the model and decreasing the errors.

Also the delay effects discussed in the estimation of the heat transfer coefficients in Section 3.5.3, and visible in Figures 19 and 18, are interesting future research topics. These effects are related to the phases inside the reactor.

It would be interesting in the future to find temperature dependent values of average properties such as ΔH_i and $C_{P,tot}$, which today are quite uncertain. Work on this has already started.

Concerning optimization, we first recommend that the quality of the end product is included in the objective function of the optimization problem, following a proper mathematical modeling of this entity. From the heuristic improvement (which we call manual optimization in the text) performed in this work, it is hard to tell which profile is the best.

It would also be interesting to study the impact of different set point curves, both pressure and temperature, on the total batch time in optimization.

Performing a complete optimization to find a solution to the dynamic optimization problem formulated in Section 4.2, using for instance the control vector parametrization approach for the solution, can give useful, and perhaps unexpected, profiles and would be very interesting.

References

[1] O. Abel, A. Helbig, W. Marquardt, H. Zwick, and T. Daszkowski. Productivity optimization of an industrial semi-batch polymerization reactor under safety constraints. *Journal of Process Control*, 10:351–362, 2000.

[2] N. Aziz and I. M. Mujtaba. Optimal operation policies in batch reactors. *Chemical Engineering Journal*, 85:313–325, 2002.

[3] L. T. Biegler, A. M. Cervantes, and A. Wächter. Advances in simultaneous strategies for dynamic process optimization. *Chemical Engineering Science*, 57:575–593, 2002.

[4] L. T. Biegler and I. E. Grossman. Restrospective on optimization. *Computers & Chemical Engineering*, 28:1169–1192, 2004.

[5] D. Bonvin. Optimal operation of discontinuous reactors - A personal view. *Journal of Process Control*, 8:355–368, 1998.

[6] D. Bonvin, B. Srinivasan, and D. Ruppen. Dynamic optimization in the batch chemical industry. *Aiche Symposium Series*, 326:255–273, 2002.

[7] A. M. Cervantes and L. T. Biegler. A stable elemental decomposition for dynamical process optimization. *Journal of Computational and Applied Mathematics*, 120:41–57, 2000.

[8] A. M. Cervantes and L. T. Biegler. Optimization strategies for dynamic systems. In C. Floudas and P. Pardalos, editors, *Encyclopedia of Optimization*, volume 4, pages 216–227. Kluwer, New York, 2001.

[9] K. L. Choong and R. Smith. Novel strategies for optimization of batch, semi-batch and heating/cooling evaporative crystallization. *Chemical Engineering Science*, 59:329–343, 2004.

[10] K. L. Choong and R. Smith. Optimisation of semi-batch reactive crystallization processes. *Chemical Engineering Science*, 59:1529–1540, 2004.

[11] C. M. da Silva and E. C. Biscaia, Jr. Multiobjective dynamic optimization of semi-batch polymerization processes. *Macromolecular Symposia*, 206:291–306, 2004.

[12] F. A. D'Angelo, L Brunet, P Cognet, and M. Cabassud. Modelling and constraint optimisation of an aromatic nitration in liquid-liquid medium. *Chemical Engineering Journal*, 91:75–84, 2003.

[13] I. Datkov, G. M. Ostrovsky, L. E. K. Achenie, and Y. M. Volin. Process optimization under uncertainty when there is not enough process data at the operation stage. *Optimization and Engineering*, 7:249–276, 2006.

[14] K. Deb, K. Mitra, R. Dewri, and S. Majumdar. Towards a better understanding of the epoxy-polymerization process using multi-objective evolutionary computation. *Chemical Engineering Science*, 59:4261–4277, 2004.

[15] M.-S. G. García, E. Balsa-Canto, A. A. Alonso, and J. R. Banga. Computing optimal operating policies for the food industry. *Journal of Food Engineering*, 74:13–23, 2006.

[16] T. Ishikawa, Y. Natori, L. Liberis, and C. C. Pantelides. Modeling and optimisation of an industrial batch process for the production of dioctyl phtalate. *Computers & Chemical Engineering*, 21:1239–1244, 1997.

[17] S. M. Khuu, J. A. Rodriguez, J. A. Romagnoli, and K. F. Ngian. Optimisation and control of an industrial surfactant reactor. *Computers & Chemical Engineering*, 24:863–870, 2000.

[18] S. M. Khuu, J. A. Romagnoli, P. A. Bahri, and G. Weiss. Dynamic simulation and control of an industrial surfactant reactor. *Computers & Chemical Engineering*, 22:S715–S718, 1998.

[19] S. Kirpatrick, C. D. Gelatt, and M. P. Vecchi. Optimization by simulated annealing. *Science*, 220:671–679, 1983.

[20] J. Lehtonen, T. Salmi, A. Vouri, and H. Haario. Optimization of the reaction conditions for complex kinetics in a semi-batch reactor. *Industrial & Engineering Chemistry Research*, 12:5196–5206, 1997.

[21] D. B. Leineweber, A. Schäfer, H. G. Bock, and J. P. Schlöder. An efficient multiple shooting based SQP strategy for large-scale dynamic process optimization, Part II: Software aspects and applications. *Computers & Chemical Engineering*, 27:167–174, 2003.

[22] P. Li, K. Löwe, H. Arellano-Garcia, and G. Wozny. Integration of simulated annealing to a simulation tool for dynamic optimization of chemical processes. *Chemical Engineering & Processing*, 39:357–363, 2000.

[23] S. Milanič, S. Strmčnik, D. Šel, N. Hvala, and R. Karba. Incorporating prior knowledge into artificial neural networks — an industrial case study. *Neurocomputing*, 62:131–151, 2004.

[24] K. Mitra, S. Majumdar, and S. Raha. Multiobjective dynamic optimization of a semi-batch epoxy polymerization process. *Computers & Chemical Engineering*, 28:2583–2594, 2004.

[25] Z. K. Nagy and R. D. Braatz. Open-loop and closed-loop robust optimal control of batch processes using distributional and worst case analysis. *Journal of Process Control*, 14:411–422, 2004.

[26] A. Nayak and S. K. Gupta. Multiobjective optimization of semi-batch copolymerization reactors using adaptations of genetic algorithm. *Macromolecular Theory and Simulations*, 13:73–85, 2004.

[27] R. H. Perry and D. W. Green. *Perry's Chemical Engineers' Handbook*. McGraw-Hill, New York, 7 edition, 1997.

[28] D. A. Pierre. *Optimization Theory with Applications*. Series in Decision and Control. John Wiley & Sons, Inc., 1969.

[29] V. Pontryagin, V. Boltyanskii, R. Gamkrelidge, and E. Mishchenko. *The Mathematical Theory of Optimal Processes*. New York: Interscience Publishers Inc., 1962.

[30] D. W. T. Rippin. Simulation of single- and multiproduct batch chemical plants for optimal design and operation. *Computers & Chemical Engineering*, 7:137–156, 1983.

[31] B. Srinivasan, D. Bonvin, E. Visser, and S. Palanki. Dynamic optimization of batch processes: II. Role of measurements in handling uncertainty. *Computers & Chemical Engineering*, 27:27–44, 2002.

[32] B. Srinivasan, S. Palanki, and D. Bonvin. Dynamic optimization of batch processes: I. Characterization of the nominal solution. *Computers & Chemical Engineering*, 27:1–26, 2003.

[33] P. Terwiesch, M. Agarwal, and D. W. T. Rippin. Batch unit optimization with imperfect modelling: A survey. *Journal of Process Control*, 4:238–258, 1994.

[34] P. Terwiesch, D. Ravemark, B. Schenker, and D. W. T. Rippin. Semi-batch process optimization under uncertainty: Theory and experiments. *Computers & Chemical Engineering*, 22:201–213, 1998.

[35] C. Toulouse, J. Cezerac, M. Cabassud, M.V. Le Lann, and G. Casamatta. Optimisation and scale-up of batch chemical reactors: Impact of safety constraints. *Chemical Engineering Science*, 51:2243–2252, 1996.

[36] O. Ubrich, B. Srinivasan, P. Lerena, D. Bonvin, and F. Stoessel. Optimal feed profile for a second order reaction in a semi-batch reactor under safety constraints experimental study. *Journal of Loss Prevention in the Process Industries*, 12:485–493, 1999.

[37] Z. Verwater-Lukszo. A practical approach to recipe improvement and optimization in the batch processing industry. *Computers in Industry*, 36:279–300, 1998.

[38] C. L. Yaws. *Yaws' Handbook of Thermodynamic and Physical Properties of Chemical Compounds*. Knovel, 2003. Online version available at: `http://www.knovel.com/knovel2/Toc.jsp?BookID=667&VerticalID=0`.

[39] V. M. Zavala, A. Flores-Tlacuahuac, and E. Vivaldo-Lima. Dynamic optimization of a semi-batch reactor for polyurethane production. *Chemical Engineering Science*, 60:3061–3079, 2005.

A Initial simulations with basic EO profiles

We start with two simulations where the same levels as in the original profile is used, but only one plateau (and hence a duration differing from the original), starting with a simulation with a plateau level as the first plateau, and then a simulation with the second plateau level. Thereafter a simulation follows, where the EO-profile has a constant slope, starting at the second plateau level and ending at the 'batch' plateau level in the original profile. A profile with three different constant levels has also been investigated below.

Figure 25 shows the simulation where EO is added at a constant level being the same as the 'batch plateau' level in the original profile. This is in reality not wanted, since the reactor temperature is too low for too long, which results in a bad end product quality. It can also be seen, in the upper left graph, that the control system does not manage to keep the reactor temperature close enough to the set point temperature. This is also seen in the objective function value, $f_{obj} = 10.57$, since the penalty $p = 10$ is activated.

Figure 26 shows the simulation where EO is added at a constant level being the same as the second plateau level in the original profile. The figure shows that the control system is able to manage a profile like this. The objective function value is $f_{obj} = 0.57$, which is slightly better than the original value. In reality this profile is not wanted, since the reactor temperature is too low during a too long time period of the EO addition, which means that a too large part of the EO is added at low temperatures, which in turn gives a bad quality to the end product. This effect ought to be added to the optimization problem, either as a constraint or as a penalty in the objective function.

We next investigate some profiles with levels different from those in the original profile. In the simulation in Figure 27, a profile with three different levels is used: the first original plateau level followed by a second, constant level equal to the original but shorter duration, and a third, somewhat lower level than the original second plateau level. As in the original profile, the reactor temperature is allowed to reach the wanted temperature before the second level starts. The objective function value is 0.62, which is just above the value for the original EO profile, and hence nothing is gained using this profile.

Figure 28 shows a simulation where EO is added with a constant slope, starting at the lower second plateau level and ending at the 'batch plateau' level in the original profile. At the beginning of the EO addition, the reactor temperature is too low for too long, which gives a bad and uneven quality to the end product. In the simulation it seems as the system almost manages the profile, but regarding the errors present in the model, the reactor temperature is close to being non useful (the reactor temperature rises very fast while the jacket temperature is the lowest possible). The objective function value is $f_{obj} = 10.59$, confirming the conclusion that this is not a recommended profile.

Now we investigate some profiles where the interval of no addition is removed. The length of the removed interval is 0.11 time units, which implies that a good guess is that we will save at least this time; the total batch time should be 0.11 time units shorter than for the original profile. A disadvantage of these profiles is that the reactor temperature is lower than wanted during a large part of the batch, which affects the quality in a bad way.

Figure 29 shows a simulation where the EO 'batch plateau' is immediately followed by the second plateau level, that is, the original profile where the interval with no addition is removed. The objective function value is $f_{obj} = 0.55$, which is better than the original objective function value, but we do not gain all the saved time. This is due to the lower reactor temperature during a part of the second, lower plateau, which results in a lower reaction rate, and a worsened quality.

The objective function value, using a profile as in Figure 30, where the EO 'batch plateau' is instantly followed by a second, somewhat lower, plateau level and a third, even lower level, is $f_{obj} = 0.55$. As above, this profile is really not wanted, due to the worsened end product quality.

All simulations and the corresponding objective function values are given in Table 9.

Table 9: Objective function values for different simulations.

Simulation (Figure)	Objective function value	Worsened quality
25	10.57	yes
26	0.57	yes
27	0.62	
28	10.59	yes
29	0.55	yes
30	0.55	yes

Two profiles of the manually tested ones give the shortest batch time, 0.55 which is 10 % lower than today, given in Figure 29 and 30. As discussed above, neither of these simulations are preferred, because of bad end product quality. All we conclude from this small investigation is that a piecewise constant function profile with two or three descending levels gives shorter batch time, and at the same time results in a worsened end product quality.

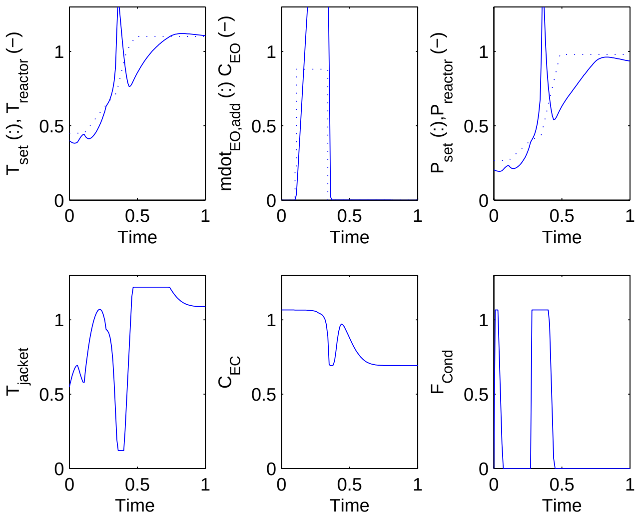

Figure 25: The figure shows a simulation where EO is added at a constant level being the same as the ’batch plateau’ level in the original profile.

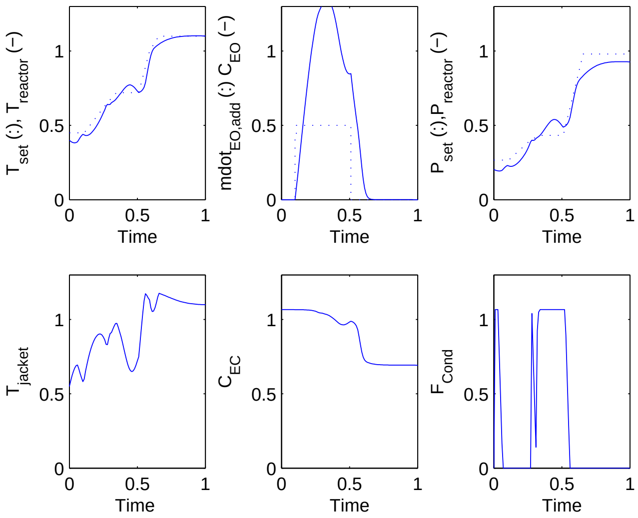

Figure 26: The figure shows a simulation where EO is added at a constant level being the same as the second plateau level in the original profile.

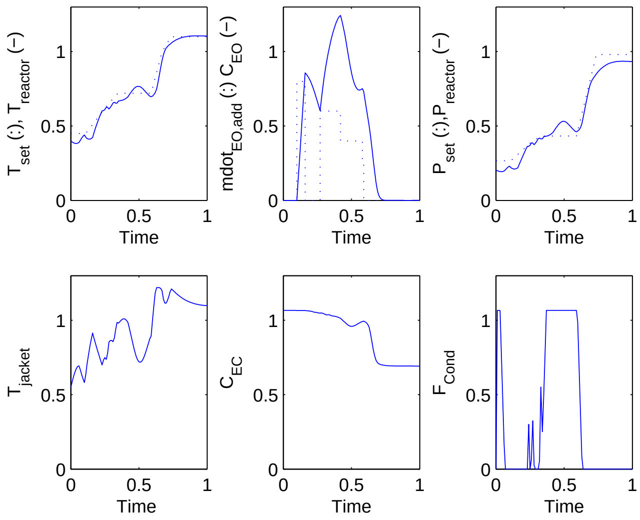

Figure 27: The figure shows a simulation where the EO 'batch plateau' is followed by a second, somewhat lower, plateau level and a third, even lower level. As in the original profile, the reactor temperature is allowed to reach the wanted temperature before the second level starts.

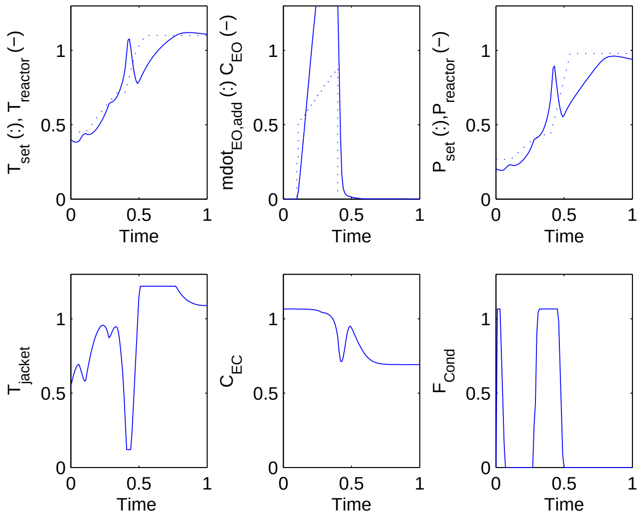

Figure 28: The figure shows a simulation where EO is added with a constant slope, starting at the second plateau level and ending at the 'batch plateau' level in the original profile.

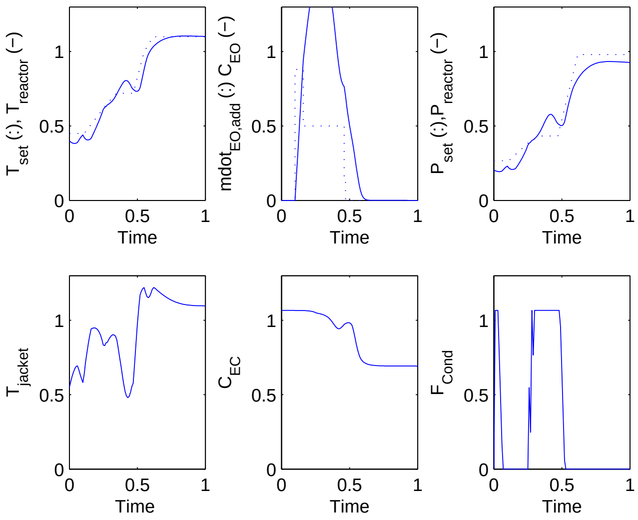

Figure 29: The figure shows a simulation where the EO 'batch plateau' is instantly followed by the second plateau level, that is, the original profile where the interval with no addition is removed.

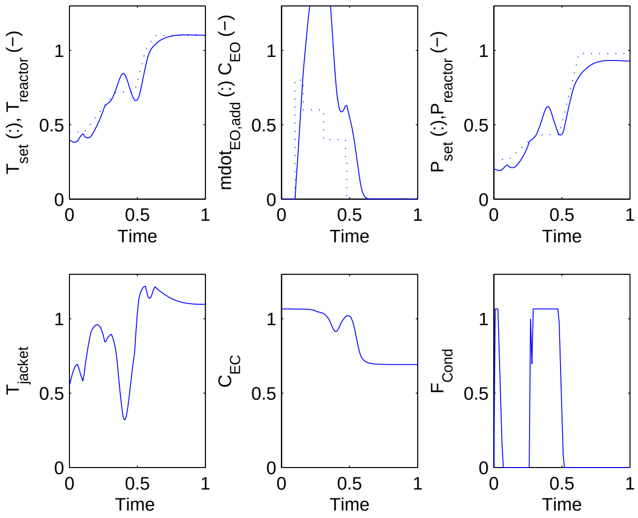

Figure 30: The figure shows a simulation where the EO 'batch plateau' is instantly followed by a second, somewhat lower, plateau level and a third, even lower level, c.f. Figure 27.